Next Materials 8 (2025) 100548

Contents lists available at ScienceDirect

Next Materials

journal homepage: www.sciencedirect.com/journal/next-materials

Review article

New challenges for lithium fluoride: From dosimeter to solid-state batteries (review)

Utkirjon Sharopov [a,b,1,*], Tukhtamurod Juraev [a], Siddik Kakhkhorov [b], Khusniddin Juraev [b], Muzaffar Kurbanov [c], Mukhtorjon Karimov [c], Dilmurod Saidov [d], Alisher Kakhramonov [e], Feruza Akbarova [e], Islomjon Rakhmatshoev [f], Odiljon Abdurakhmonov [g]

[a] Physical-Technical Institute, Uzbekistan Academy of Sciences, Tashkent, Uzbekistan
[b] Bukhara State University, Bukhara, Uzbekistan
[c] Urgench State University, Urgench, Uzbekistan
[d] Urgench Ranch University of Technology, Urgench, Uzbekistan
[e] Institute of Materials Science, Uzbekistan Academy of Sciences, Tashkent, Uzbekistan
[f] Fergana Polytechnic Institute, Fergana, Uzbekistan
[g] Tashkent Institute of Chemical Technology, Tashkent, Uzbekistan

ARTICLE INFO

Keywords:
Lithium fluoride (LiF)
Material science
Applications
Surface
Dosimetry
Solid electrolytes

ABSTRACT

Lithium fluoride (LiF) stands out as a material with exceptional physical and chemical properties, including high ionic conductivity, thermal stability, and compatibility with modern battery components. While its initial applications were rooted in radiation dosimetry due to its thermoluminescent capabilities, LiF has since evolved into a versatile material with broad applications spanning optics, electronics, and lithium-ion battery (LIB) technologies. This review delves into the multifaceted roles of LiF, charting its progression from a dosimetric material in the 1980s to a critical component in next-generation solid-state batteries. The material's ability to enhance the stability, durability, and safety of LIB components, especially in solid electrolyte systems, is particularly emphasized. LiF also plays a significant role in the fabrication of high-efficiency OLED devices, as well as in nuclear technologies, where it is utilized in neutron dosimetry and reactor materials. Furthermore, the paper explores LiF's contributions to defect engineering, surface modifications, and recycling strategies, which are pivotal in advancing its application in energy storage technologies. Beyond batteries, LiF's utility extends to fields like catalysis, biomedicine, and nuclear technologies, reflecting its vast potential for future innovations. This study provides a comprehensive overview of LiF's properties, applications, and research directions, offering insights into its critical role in the development of sustainable and high-performance materials for emerging technologies.

1. Introduction

Today, the fourth generation of lithium-ion technology with enormous potential is on the verge of further development. Due to its unique properties and advantages, such as inherent safety, high ionic conductivity, chemical stability and compatibility, economic potential, and non-proliferation in nature, LiF has become the focus of significant attention for lithium-ion technology [1–3].

Historically, the use of LiF began in radiation dosimetry, where its thermoluminescent properties enabled precise measurement of ionizing radiation doses [4]. Later, with the advancement of technologies, lithium fluoride found widespread application in the optical industry, nuclear technologies [5], electronics [6], and modern lithium-ion batteries (LIBs) (Fig. 1). Recent studies show that the addition of LiF to electrolyte and cathode materials significantly enhances their stability, durability, and safety, which is particularly critical for the development of solid electrolytes in lithium-ion technologies. Additionally, LiF is actively utilized in medical applications, including radiation detectors, as well as in the foundry industry due to its ability to withstand extreme temperatures and chemical exposure.

* Correspondence to: "Solar thermal and power plants" laboratory, Physical-Technical Institute, Chingiz Aitmatov St., 2, Tashkent 100084, Uzbekistan.
E-mail address: utkirstar@gmail.com (U. Sharopov).
[1] https://orcid.org/0000-0002-7962-0426

https://doi.org/10.1016/j.nxmate.2025.100548
Received 24 August 2024; Received in revised form 1 February 2025; Accepted 13 February 2025
Available online 20 February 2025

This article examines the main areas of research and application of LiF over the past 50–60 years, ranging from optics and electronics to nuclear technologies, LIBs, medicine, and industry. A detailed analysis not only highlights the advantages of LiF but also identifies promising directions for further research and the development of innovative technologies based on this material.

This study primarily reviews the history of research on LiF materials, including authors and active research centers. Then, the research status of LiF is presented, describing the current state of research, the scientific areas in which LiF is used, and the strategy of experimental research. In addition, the resulting novelties and challenges encountered when using LiF are discussed, including defect formation in materials, optimization of solid electrolyte component systems for energy control, interactions with other substances, and disposal and recycling methods. Based on the above, research directions in the field of LiF are discussed, and research areas are recommended for the future development of Li-ion and other technologies. The purpose of this article is to provide the current state of research and expected future developments in the field of LiF-related materials.

2. Methodology

To achieve our goal, we employed a content analysis approach based on the survey method. An extensive literature search was conducted across various platforms, including Scopus, Web of Science, Science Direct, Google Scholar, ResearchGate, and international agencies.

Of course, we cannot cover the entire spectrum of existing crystals, which includes metals, semiconductors, and alkali halide crystals. Doing so would result in an overwhelming amount of data that would require extensive processing. However, among all classes of crystals, alkali halide crystals hold a special place due to their unique properties and wide range of applications.

Comprehensive searches were conducted using keywords such as: “lithium fluoride (LiF); surface of alkali halide crystals; surface of lithium fluoride crystals; defects in lithium fluoride crystals; lithium fluoride in solid-state batteries; lithium fluoride in solid electrolytes; issues, advantages, and applications, as well as pros and cons.”

During this search process, numerous articles were identified. The literature evaluation involved a thorough analysis of titles, keywords, abstracts, article contents, and journal topics to select relevant references.

The review process was carried out in two distinct stages:

- Selection Method
- Review Results

The selection stage began with an extensive literature search, during which several dozen documents were identified. Subsequent evaluation, including key keywords and an assessment of titles, abstracts, topics, and materials, narrowed down the selection. Finally, factors such as impact factor, citation count, review process, and publication period were considered, leading to the selection of appropriate articles. These articles formed the basis for subsequent review, analysis, and critical discussion of lithium fluoride materials used in various industries. The topics discussed included an overview and comparison of properties and functions for use in different applications, the growing demand for such

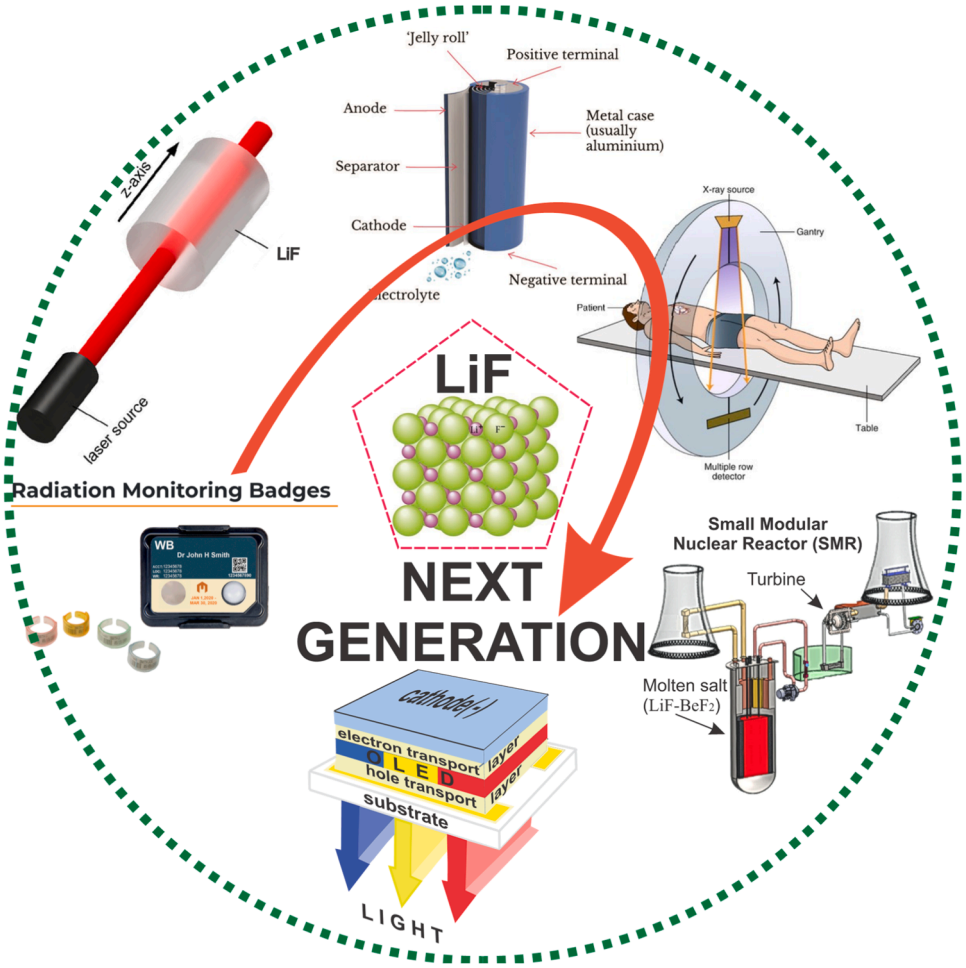

Fig. 1. The Evolution of Lithium Fluoride Applications: From Dosimetry to Future Technologies.

materials, structure, classification, advantages, optimization of various applications, as well as general issues.

Following this, research directions and potential areas for future research to advance various technologies related to LiF materials are discussed.

3. Brief information about lithium fluoride crystals

Lithium fluoride crystals are distinguished by their unique properties. These crystals exhibit a cubic crystal structure similar to that of NaCl. LiF crystals belong to the cubic system, which provides them with high symmetry and an orderly atomic arrangement (Fig. 2).

Under normal conditions, lithium fluoride exists as a white powder or transparent, colorless crystals with a cubic symmetry. Its space group is Fm3m, with atomic parameters of $a = 0.40279\ nm$ and $Z = 4$. It melts at a temperature of 848.2 °C. Lithium fluoride is a diamagnetic material with a molar magnetic susceptibility of -10.1×10^{-6} cm^3 /mol.

Electrons in LiF crystals are distributed across energy zones and bands. Due to the ionic bonds between lithium and fluoride ions, this material exhibits the properties of an electrical insulator. The fluorine atom accepts one valence electron from lithium, forming an F^- ion with eight valence electrons.

The physicochemical properties of LiF crystals are characterized by their high stability and durability. These crystals are thermally stable, chemically inert, and exhibit excellent optical transmission capabilities. Such properties make lithium fluoride highly sought after in various fields, including optics, electronics, and precision scientific instruments.

Lithium fluoride demonstrates exceptional transparency across a wide range of wavelengths, from ultraviolet to infrared radiation (0.12–6 μm). As a result, it is extensively used in ultraviolet optics (including vacuum ultraviolet, where its transparency surpasses that of all other optical materials) and infrared optics. Additionally, lithium fluoride is employed in radiation dose measurements using thermoluminescent dosimetry (TLD) methods.

Monocrystals of lithium fluoride are used in X-ray monochromators and in the development of lasers with highly efficient (up to 80 %) color centers. Lasers based on F_2^- centers emit infrared radiation with a wavelength of 1120 nm. Lithium fluoride exhibits weak scintillation. With a wide bandgap of 12 eV, LiF has high specific electrical resistance.

4. Results and discussion

Data obtained from the Scopus and Science Direct search systems indicate that after the 1940s, during World War II, alkali halide crystals, including LiF, became popular research subjects. This surge in interest was driven by several factors. Table 1 presents some of the reasons why these crystals were considered "trendy" for research during that period.

Alkali halide crystals, including LiF, were actively studied for the development of optical systems due to their superior transparency in the ultraviolet and infrared ranges compared to most available materials. This was crucial for military, optical, and scientific applications. As evident, the post-war trend of researching alkali halide crystals was driven by the combination of their unique properties and the pressing needs of the time. From nuclear technologies to optics and quantum physics, these materials became catalysts for numerous scientific discoveries and technological breakthroughs.

Table 1
Key reasons for the popularity of alkali halide crystals (including LiF) for research in the second half of the 20th century.

Category	Description	Examples and Reasons
Nuclear Technologies	Development of nuclear energy and dosimetry technologies.	Use of LiF in molten salt nuclear reactors. Radiation dosimetry: precise measurement of ionizing radiation doses due to thermoluminescent properties.
Optical Research	High transparency and nonlinear optical properties.	Transparency in UV and IR ranges for optical systems. Study of color centers and photorefractive effects for lasers and optical instruments.
Fundamental Physics	Investigation of defects and quantum-mechanical phenomena.	Convenient model for studying defects (vacancies, color centers). Exploration of electronic states and light-matter interactions.
Military Applications	Materials for military technologies resistant to radiation.	Active media for lasers and detectors. Space technologies: thermal protection and optical instruments.
Ease of Use	Ease of growth and processing of alkali halide crystals.	Ability to produce large, high-quality single crystals. Simple cubic structure makes them ideal as model objects.
Advancement in Research Methods	New experimental and theoretical approaches.	Use of spectroscopy (IR and UV) to analyze optical properties. Early models for computer simulation in solid-state physics.

The development of radiation-resistant materials and devices for nuclear reactors, space technologies, and dosimetry (radiation monitoring) required fundamental research into defect formation. Lithium fluoride became a model material for such studies due to its simple cubic structure and high sensitivity to radiation.

4.1. LiF in optics and electronics

During implantation, the bombardment of a surface with high-energy ions can lead to the creation of primary defects, the formation of new phases, changes in the chemical composition and structure of the surface, and even alterations in the bulk of the materials. Plasma and laser processing can also lead to melting, evaporation, decomposition of the surface material, changes in the chemical composition, structure, and topography of the surface, as well as the formation of new functional groups and structures and changes in properties.

Thus, the primary result of surface formation from physical and chemical treatments is the creation of defects. With increasing time and intensity, these treatments lead to the accumulation and increase in the concentration of defects on the surface, which will undoubtedly affect its properties. Defects in the near-surface region can have both positive and negative effects on the properties of materials. For example, they can affect mechanical strength, electrical conductivity, optical

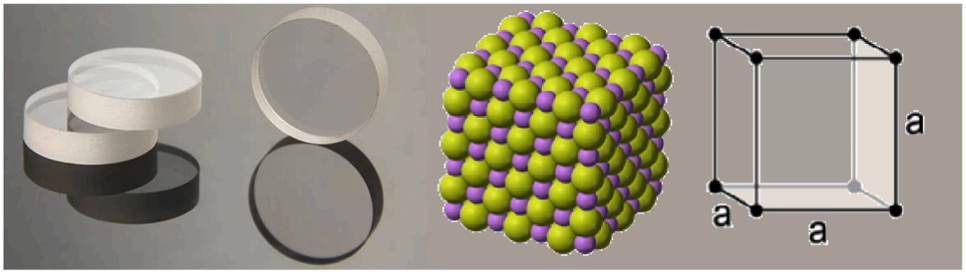

Fig. 2. Appearance, atomic arrangement of LiF, and cubic crystal structure.

characteristics, catalytic properties, corrosion resistance, etc.

This section analyzes key achievements and current challenges related to the study of defects in LiF that affect its luminescent properties, including fluorescence, photoluminescence (PL), and thermoluminescence. Since thermoluminescence (dosimetry) in LiF is an extensive and significant topic, a separate paragraph will be dedicated to it in the following section.

Recent data obtained from the Scopus and ScienceDirect search systems revealed an unusual trend based on studies on the surface of alkali halide crystals and specifically LiF crystals (Fig. 1). As shown in Fig. 1, the number of studies conducted on the surface of alkali halide crystal samples per year until 2024 is illustrated. After 2000, the number of experimental and theoretical works carried out sharply decreases, reaching approximately 50 works per year, whereas in 1996, the number reached 125 works (Fig. 3, red line).

However, if we search for publications specifically on the surface of LiF crystals, we observe the following trend shown by the red line in Fig. 3. There is a sharp increase in the number of publications (by about 20 times) related to experimental and theoretical work on the surface of LiF. This surge is primarily due to the increased use of these materials as a key component of solid electrolytes for LIBs [7].

Apart from its use in LIBs, LiF also finds applications in other fields such as optics [8], catalysis, and biomedicine. Fig. 4 shows that after the 1980s, most research on the LiF surface was conducted for use in dosimetry, nuclear energy, and nuclear medicine. After the 1990s, the graph indicates increased use in laser technology for optical applications. From the 2000s onward, as shown by the red line, LiF has primarily been used as an electrolyte in LIBs, highlighting the growing interest and publications in this area.

Indeed, from the presented graph, it can be seen that after the 1980s, the number of studies on the LiF surface increased significantly since LiF is an ideal material for dosimeters. It can accurately measure X-ray [9] and gamma radiation doses [10], making it a valuable tool for monitoring radiation exposure in various fields such as medicine, electronics, nuclear power, industrial, and space materials science.

In the 1990s, LiF was such a popular material that entire scientific groups conducted research on it. One notable group is the laboratory led by Rosa Maria Montereali at the ENEA Institute - Frascati Research Center. To date, this group has published more than 300 articles devoted to LiF materials. In Fig. 5, you can see the number of articles by author dedicated to research on the surface of LiF crystals. Additionally, Horowitz, Yigal S. from the Israeli Ben-Gurion University, is still publishing on the topic of thermoluminescence in LiF dosimeters, and their number of publications is increasing (more than 100 publications).

Significant contributions to the study of the optical properties of LiF crystals when exposed to radiation were made by RM Montereali, F. Bonfigli, and E. Nichelatti. They are leading specialists in the field of studying the physicochemical properties of LiF crystals, conducting extensive research on the luminescent properties of LiF crystals activated with various impurities under different types of radiation. They have also studied second harmonic generation, photorefraction, and other nonlinear optical phenomena in LiF crystals.

By the beginning of 2010, their research group had accumulated a vast amount of data on defects in LiF, their absorption, and PL (see Fig. 6). Their research has shown that these defects can be utilized in creating lasers in thin films and crystals (see Fig. 7).

Fig. 4 displays the absorption and emission spectra of several color centers (CCs) (F_2, F_3^+ F_2^+ etc.) in LiF crystals at room temperature (RT). These peaks indicate that color centers absorb light at specific wavelengths and emit light at specific wavelengths after absorption.

Fig. 7 illustrates the relationship between the average energy and tuning range of CC lasers operating at room temperature in pulsed mode in LiF crystals. The tuning range refers to the wavelengths that the laser can be adjusted to emit. These figures collectively suggest that CCs in LiF crystals can serve as sources for wavelength-tunable lasers. The specific laser wavelength and tuning range vary depending on the type of CC

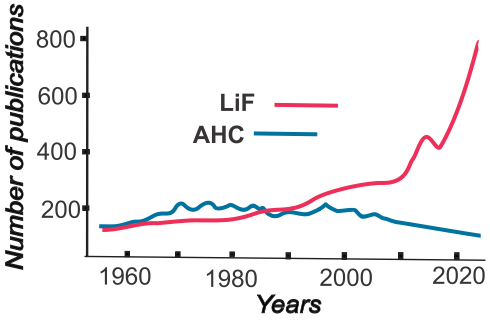

Fig. 3. Number of publications devoted to processes on the surface of alkali halide crystals (AHC) (red) and lithium fluoride (blue) over time.

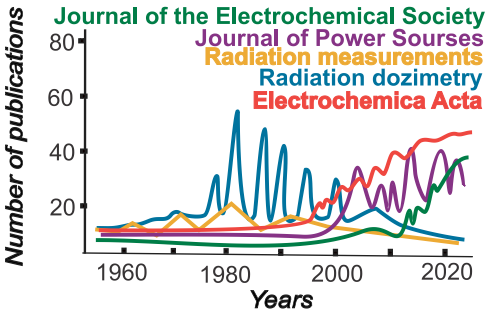

Fig. 4. Number of publications from various scientific sources concerning the surface of LiF crystals over time.

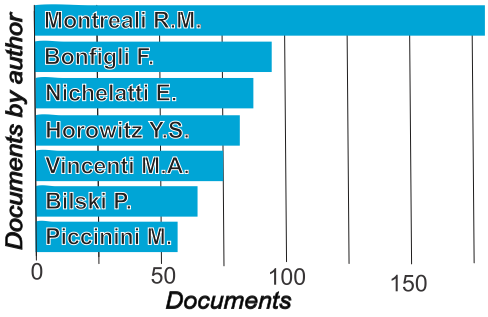

Fig. 5. Number of publications by author over the entire period devoted to research on the surface of LiF crystals.

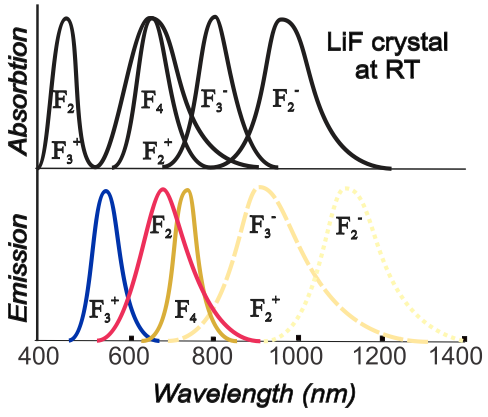

Fig. 6. Absorption and emission bands, outlined as normalized Gaussian curves, of the known CCs which possess PL in LiF at RT. Reproduced from [11] with permission.

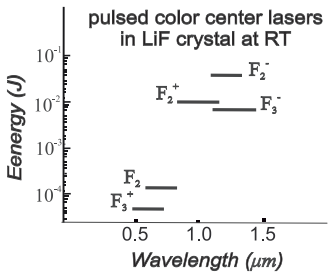

Fig. 7. Average energy and tunability range versus wavelength of the CC lasers operating at RT in LiF crystals in pulsed regime. Reproduced from [11] with permission.

employed.

By the beginning of 2010, tables detailing defects in LiF were compiled based on research data from this group. All the data obtained are presented in Table 2.

The Table 2 contains the spectroscopic properties and room temperature optical gain of laser-active CCs in LiF grown by non-stoichiometric crystal growth at n = 1.39.

Explanation of the table:

λ_a (nm): Absorption wavelength of the CC.

λ_e (nm): Emission wavelength of the CC after absorbing light.

$\Delta\nu$ (10^{13} Hz): Energy difference between the absorption and emission states of the CC in units of 10^{13} Hz, related to the emitted light color.

τ_{eff} (ns): Effective lifetime of the excited state of the center, indicating how long the electron stays in the excited state before returning to the ground state.

η (%): Quantum yield of the CC, the percentage of absorbed photons converted into emitted photons.

g (cm^{-1}): Optical gain of the CC, indicating how much light is amplified when passing through the material.

Overall, the table demonstrates that defects in LiF crystals can serve as active media for lasers, with specific properties varying depending on the type of CC.

Their work has significantly contributed to understanding luminescence mechanisms, clarified the role of defects in the optical properties of LiF crystals, and opened new possibilities for their use in nonlinear optics. They conducted comprehensive studies on PL, electroluminescence, and thermoluminescence of LiF crystals with defect states. Additionally, LiF radiation detectors, based on the thermoluminescence method, exhibit a response where the luminescent detector's efficiency depends on the received dose magnitude, the detector's composition materials, and the method of dose transmission (i.e., the microscopic pattern of energy release), greatly affecting its effectiveness [12]. Lithium fluoride detectors have high sensitivity to ionizing radiation and are capable of detecting α, β, γ radiation, as well as η and ρ particles [13].

LiF detectors demonstrate a highly linear response to radiation intensity and have low background noise, enabling accurate measurement of radiation doses under diverse conditions. Additionally, LiF exhibits resistance to thermal and mechanical stress, ensuring reliability and durability in operation [14]. Its low cost, ease of processing, and usability make LiF a preferred choice for a wide range of applications, from personal dosimetry to scientific research and radiation monitoring in fields such as medicine, nuclear power plants, and space exploration. In contrast, other materials may be less convenient and mobile, limiting their application to narrow fields of science and technology [15]. For example, some materials may be heavy or require complex cooling systems or specific environmental conditions [16], restricting their use in mobile or field settings [17]. LiF, due to its lightweight nature, convenience, and ease of use, enjoys widespread adoption. Recent research [18] has also shown that LiF has potential applications in UV dosimetry.

Table 2
Spectroscopic properties and optical gain at room temperature of laser-active CCs in LiF.

CCs	λ_a (nm)	λ_e (nm)	$\Delta\nu$ (10^{13} Hz)	t_{eff} (ns)	η (%)	g(cm^{-1})
F_3^+	448	541	6.5	11.5	100	7.6
F_2	444	678	7.5	17	100	7
F_3^-	800	900	8	10	10	1.9
F_2^+	645	910	7	15	50	7.6
F_2^-	960	1120	8	55	30	1.6

Now, let's examine key studies from the last 5 years. In [19] visible PL of CCs in LiF crystals was studied for advanced diagnostics of 18 and 27 MeV proton beams. Using a simple defect formation model that considers energy release in the material and saturation of defect concentration, researchers obtained a two-dimensional dose map from the image of transverse beam intensity distribution. They also reconstructed the full Bragg curve, enabling comprehensive characterization of proton beams produced by the accelerator. The high intrinsic spatial resolution and wide dynamic range of these new LiF detectors facilitated two-dimensional imaging of lateral beam intensity distribution. These findings are crucial for dose assessment in hadron therapy and for nuclear and space research at CERN (European Organization for Nuclear Research) [20].

In [21], a comparative study of PL and modeling of F_2 and F_3^+ CCs in lithium fluoride irradiated at high doses with low-energy proton beams was conducted. In their work, the authors studied the PL of F_2 and F_3^+ CCs in lithium fluoride crystals irradiated with a proton beam with energies of 3 and 7 MeV (Fig. 6). Radiation doses varied from $10^3 \div 10^6$ Gy. Ionization caused by protons in LiF crystals led to the stable formation of CCs exhibiting broad PL bands in the red (F_2) and green (F_3^+) regions of the spectrum when optically pumped with blue light (~450 nm).

The main goal of the study was to investigate the dependence of PL intensity on the absorbed dose. It was found that at high doses (about $10^6 \div 10^7$ Gy) there is a decrease in the integral PL intensity for F_3^+ centers. The authors suggest that this phenomenon is associated with the formation of absorption or quenching centers that absorb or scatter PL. The study covers a wide range of radiation doses, allowing for a detailed examination of the effects that occur at different levels of radiation exposure. The work offers a separate analysis of the contribution of F_2 and F_3^+ CCs to the overall PL, contributing to a better understanding of the processes occurring in irradiated LiF crystals.

The results may be useful for improving diagnostic and dosimetry techniques in radiation therapy, especially in the context of the use of protons and other heavy particles. In this work, there is a discrepancy between the model and the experimental data at low irradiation doses, which may be due to measurement inaccuracies or nonlinear effects of the formation of CCs. Additionally, the model used does not always accurately describe the behavior of the system, especially at high doses, which requires further research and possible modification of theoretical approaches.

The authors of the study [22] from ENEA studied the visible PL of CCs in thin films of lithium fluoride for use in detectors of low-energy proton beams at high doses. The article describes how irradiation of thermally evaporated LiF thin films with a proton beam with a nominal energy of 3 MeV in the fluence range from $10^{11} \div 10^{15}$ protons/cm^2 causes the formation of stable CCs, including primary F centers and aggregate defects F_2 and F_3^+. The authors showed that PL, measured in spectrally integrated form, depends on the absorbed dose and behaves linearly until saturation at high dose values ($>\approx 10^5$ Gy). It was found that the spectral contributions of F_2 and F_3^+ CCs in the red and green regions of the spectrum exhibit differences in their behavior at high irradiation doses.

The difference between this work and the previous one is that thin LiF films provide high spatial resolution, which is important for accurate mapping of radiation doses. The study also demonstrates the detectors' ability to operate in a wide range of doses, from low to high values, making them versatile for various applications. It has been shown that CCs remain stable at room temperature, simplifying their use and

analysis. After irradiation, the detectors do not require complex processing, facilitating their operation.

This work does not take into account the influence of the proton beam energy on the formation of CCs, which requires consideration when calibrating detectors for various irradiation conditions. Additionally, the limited thickness of LiF films (about 1 μm) can affect their ability to detect deeper layers of materials, and signal saturation at high doses limits the capabilities of detectors under extremely high radiation doses. This necessitates further research to expand their applicability. However, ultimately, this and other studies from this group [23] demonstrate the promise of using LiF thin films to detect low-energy proton beams, offering new opportunities for radiation diagnostics and therapy while indicating the need for further research to optimize their performance and expand the range of applications.

In [24], solid-state radiation detectors using PL of stable point defects in LiF crystals were employed for advanced diagnostics during the commissioning of the TOP-IMPLART linear proton accelerator segment with energies up to 27 MeV for proton therapy. Here, LiF detectors provided high spatial resolution and a wide dynamic range, enabling the creation of two-dimensional images of the transverse distribution of beam intensity. They also accurately determined the position of the Bragg peak using a conventional optical fluorescence microscope. The term "Bragg peak" in the context of radiation therapy refers to the specific point within a material where maximum energy release from ionizing radiation, such as protons, occurs. This peak is displayed on a graph of absorbed dose versus radiation penetration depth. The critical point is that most of the radiation energy is released just before the particles come to a complete stop.

The study reports and discusses the results of proton beam characterization, including estimates of energy components and beam dynamics under various accelerator operating conditions. Fig. 9 shows the dependence of PL intensity on the depth of proton penetration into LiF. Protons with an energy of 27 MeV are used to excite PL. The work shows that the intensity of PL in LiF depends on the depth of proton penetration. The maximum PL intensity is achieved at a certain penetration depth, after which it gradually decreases.

The continuation of this work allowed [25], based on this knowledge, the creation of solid-state dosimeters based on PL readings. The authors conducted a systematic study of the optical properties of LiF when exposed to 7 MeV proton beams and found that the PL of these CCs under optical pumping is proportional to the absorbed dose. A model was developed to reconstruct the Bragg curve and perform 2D dose mapping from PL images stored in LiF. The study presents results highlighting quantitative aspects of PL behavior in LiF at various doses, including cases of high CC saturation.

The fourth most prolific author in publications on LiF surface

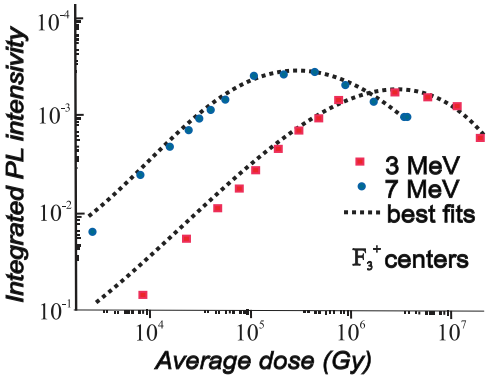

Fig. 8. PL intensities were measured for several absorbed doses emitted from spots irradiated with protons with energies of 3 and 7 MeV. Here, the PL intensities are integrated over the F_3^+ emission band, and the doses are averaged over the irradiated volume. Reproduced from [21] with permission.

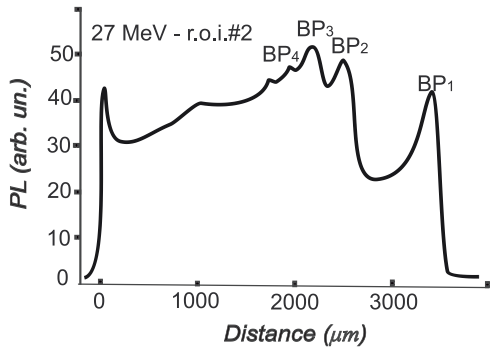

Fig. 9. PL intensity profile vs. proton penetration depth to LiF. Reproduced from [24] with permission.

research is Y.S. Horowitz and his group (Fig. 5). Horowitz specializes in studying the effects of radiation on LiF crystals [26]. He has conducted several studies on the impact of various types of radiation on the optical properties of LiF crystals [27]. Horowitz's work is important for understanding the radiation resistance of LiF crystals [28] and their potential use in radiation-resistant optical devices [29,30].

M.A. Vincenti studies the photochemical properties of LiF crystals [31]. He has conducted a number of studies on the photochemical reactions occurring in LiF crystals under the influence of various types of radiation [32]. Vincenti's work is very important for understanding the photostability of LiF crystals and their potential use in photochemical devices [33]. He and his co-authors are the first to show promising results using LiF crystals as solid-state fluorescent nuclear tracking detectors under typical ion radiobiology conditions, and further experiments are ongoing to improve this promising application, especially at higher doses and energies.

These are just a few of the many authors who have made significant contributions to the study of the optical properties of LiF crystals when exposed to radiation. The studies of these authors have helped to clarify the fundamental mechanisms underlying the optical properties of LiF crystals and opened up new possibilities for the use of these materials in various fields such as optics [34,35], laser technology [36], and medicine. It is important to note that the list of authors presented above is not exhaustive. Many other researchers have made significant contributions to this area. Apart from these main applications, LiF surface research is also being carried out in other fields such as electronics [36–38], and catalysis [39]. Due to its high sensitivity to radiation, LiF can detect very low levels of radiation [40–42], making it an attractive material for research.

Despite the significant amount of research dedicated to defect formation in the near-surface region, many issues remain insufficiently studied. To develop effective methods for defect management, a deeper understanding of their formation mechanisms and their impact on material properties is required. The development of materials with tailored surface properties could lead to the creation of new materials with unique characteristics, which in turn could stimulate the growth of various industries and improve the environmental situation. Control over defect formation in the near-surface region can enhance the efficiency of material and product production, reduce the number of defects, and increase their competitiveness. The development of new materials with improved characteristics can improve people's quality of life. For example, materials with higher corrosion resistance can be used to build more durable buildings and structures, while materials with enhanced biocompatibility can be used to create more advanced medical implants.

Overall, the study of defect formation in the near-surface region is a pressing scientific, technical, economic, social, and environmental issue. Based on this, in this paragraph, we have thoroughly analyzed the works carried out throughout the research period on defect formation and its

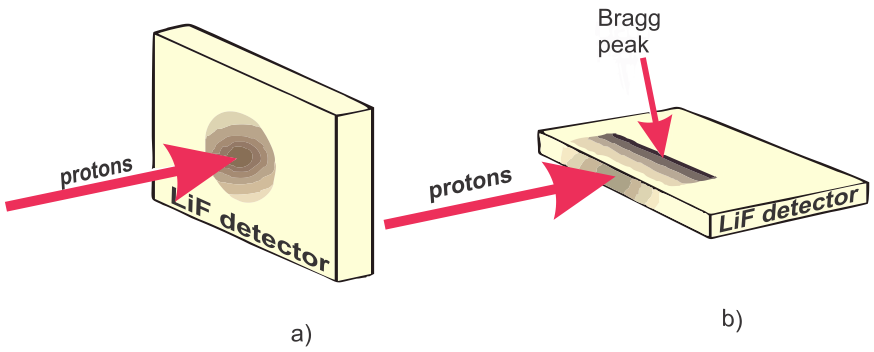

Fig. 10. Sketches of the two mounting geometries used for low-energy proton irradiation of LiF detectors: a) larger surface perpendicular to the proton beam propagation direction, b) larger surface parallel to the proton beam propagation direction. Reproduced from [25] with permission.

influence on material property changes. Alkali-halide crystals attract the attention of scientists due to their ability to easily form and modify defects under the influence of external factors, which opens up possibilities for targeted control of their properties. These crystals, including materials such as NaCl and LiF, are widely used in various fields of science and technology, from optics and electronics to biomedicine and nuclear energy. The data obtained from research on defects in alkali-halide crystals are of great importance not only for the development of technologies based on these materials but also for a broader understanding of defect formation processes in other classes of crystals, such as semiconductors and metals. Since the mechanisms of defect formation and evolution are largely universal, the results obtained in alkali-halide crystals can be adapted to interpret similar processes in semiconductors and metals. This allows for the use of accumulated knowledge to improve material properties in electronics, where defects play a key role in determining conductivity and longevity, as well as in metallurgy, where defect management is crucial for mechanical properties and corrosion resistance. Thus, in-depth study of defect formation in lithium fluoride crystals opens new prospects for interdisciplinary application and technology advancement, representing a promising direction capable of bringing significant scientific and technical achievements. Due to its many advantages, LiF is likely to remain an important material for research and development for many years to come.

4.2. LiF in dosimetry

As stated above, when radiation affects the surfaces and the bulk of LiF, different types and quantities of defects are formed, which can be used to create lasers and modify the electronic and optical properties of the material. Additionally, lithium fluoride plays a crucial role in TLD, providing accurate radiation dose measurements due to its ability to efficiently accumulate and release energy when exposed to radiation. These unique properties make LiF an indispensable component for solving a range of tasks in nuclear physics and related technologies [43].

As demonstrated in the previous paragraph, the study of luminescence mechanisms and the role of defects in forming the optical properties of LiF crystals has opened new opportunities for developing dosimeters based on the thermoluminescence effect in LiF crystals. [12]. It follows that a precise understanding of these changes in efficiency is fundamental. For the design of dosimeters based on fluorescent detectors, it is essential to accurately assess the measured radiation doses. Below, in Table 3, we have compiled various methods of radiation detection.

Table 3 highlights the materials used in various radiation detection methods, providing insights into which materials are effective at detecting certain types of radiation and under what conditions they are used.

The Table 3 emphasizes the significant advantages of LiF detectors. LiF detectors offer high sensitivity to ionizing radiation and can detect various types of radiation, including α, β, γ radiation, and neutrons [13]. Radiation detectors are most commonly used as dosimeters, and one of the simplest and most widely used methods for radiation detection is TLD.

TLD is a method for measuring and recording doses of ionizing radiation using materials that can accumulate radiation energy. When these materials are heated, the accumulated energy is released in the form of light (thermoluminescence), the intensity of which is proportional to the radiation dose received. This method is widely used in

Table 3
Various methods for recording radiation.

Method	Description and principle of work	Type of radiation	Basic materials	Applications
Geiger-Muller counter	Radioactive particles ionize the gas, creating an electrical impulse.	α, β, λ	Gas (argon, helium, neon)	measuring radiation levels
Scintillation	They emit light when they absorb a radioactive particle. Light is converted into an electrical signal.	α, β, λ, η	NaI, CsI, BGO, plastics, liquid scintillators	Medical diagnostics, particle physics
Ionization camera	Measures the current produced when a gas is ionized by radiation in an electric field.	α, β, λ	Gas (usually air or argon)	Radioecology, medical physics
Proportional counter	Similar to an ionization chamber, but amplifies the signal to be proportional to the amplitude of the energy of the ionizing event.	α, β, λ	Argon gas with methane admixture	Spectrometry, scientific research
Semiconductor	Radiation creates electron-hole pairs, generating an electrical signal.	α, β, λ	Si, Ge, GaAs	High precision spectrometry
Thermoluminescent	The material stores energy from radiation and releases it as light when heated.	α, β, λ, η, ρ	LiF, CaF_2	dosimetric equipment
Electron spin resonance	Measures the change in the state of electrons in materials caused by radiation.	α, β, λ	Amino acids, carbonates, quartz	Dosimetry, radiation biology
Bubble camera	A liquid in a superheated state forms bubbles along the trajectory of charged particles.	particles	Liquid hydrogen, liquid neon	Experimental physics
Spark camera	Sparks are created in a gas along the tracks of charged particles in an electric field.	particles	Gas (usually argon or a mixture of gases)	Experimental physics

radiation protection, medical diagnostics, radiation therapy, and environmental research. In Table 4, you can find materials used for thermoluminescent dosimeters (TLDs) and their main characteristics.

As shown in the Table 4, lithium fluoride is one of the most versatile materials for TLD. Thanks to various doping options, such as LiF:Mg,Ti (e.g., TLD-100, TLD-700) [44], LiF:Mg,Cu,P (e.g., TLD-700H, TLD-100H) [45], and LiF:Mg,Ti enriched with different lithium isotopes (6Liˆ6Li and 7Liˆ7Li), LiF is capable of detecting a wide range of radiation types, including gamma, X-ray, beta, and neutron radiation.

LiF:Mg,Ti (e.g., TLD-100, TLD-700) — This is the most widely used dosimeter with universal sensitivity to various radiation types. Enrichment with 6Liˆ6Li or 7Liˆ7Li allows the material to effectively capture neutrons, making it useful for radiation protection and medical dosimetry.

LiF:Mg,Cu,P (e.g., TLD-700H, TLD-100H) — This material features high sensitivity and low signal fading, making it suitable for precise dosimetry, especially in low-dose environments.

LiF enriched with 6Liˆ6Li (e.g., TLD-600) — This is used for neutron dosimetry, making it an important tool in nuclear energy and reactor applications.

Thus, LiF is one of the most preferred materials for dosimetry due to its versatility, high sensitivity, and ability to be used across various fields, including medical dosimetry, radiation protection, and neutron radiation monitoring. Below, Table 5 summarizes the types of radiation detected by lithium fluoride and their characteristics.

As seen in Table 5, lithium fluoride is a highly effective material for detecting various types of ionizing radiation. It can register a wide range of radiation, including gamma rays, X-rays, beta radiation, neutrons, alpha particles, and cosmic radiation. Due to specific defects in its crystal lattice, activated LiF materials exhibit high thermoluminescent intensity. The effective atomic number of LiF (Zeff = 8.14) is close to that of human soft tissue, enabling accurate dosimetric data for medical applications [46]. Additionally, LiF is resistant to mechanical stress and can be reused multiple times in dosimetry. It demonstrates stable responses to different radiation types and energy levels, making it a versatile material for measurements. Below, Table 6 presents various types of thermoluminescent dosimeters (TLD) based on LiF and their main characteristics.

From Table 6, it is evident that LiF compositions differ in the isotopic composition of lithium:

1. **Natural lithium fluoride** (as in TLD-100) is sensitive to all types of radiation.
2. **Enriched 7Li** (as in TLD-700) is insensitive to neutrons [47].
3. **Enriched 6Li** (as in TLD-600) is used for neutron dosimetry [48].
4. **Dopants** (e.g., Mg, Ti, Cu, P, Dy) determine the material's sensitivity to specific doses and types of radiation.
5. **Materials without lithium** (e.g., $CaSO_4$:Dy, Al_2O_3:C) are used where high sensitivity to gamma or X-ray radiation is important [49].

The disadvantages of LiF-based dosimeters include signal degradation over time, which must be accounted for during long-term measurements. Sensitivity may also be insufficient at very high or low doses. Additionally, excessively high or low doping concentrations can reduce the material's efficiency.

Thus, LiF remains one of the most universal and widely used materials in TLD due to its chemical stability, tissue equivalence, and high sensitivity. However, further research is necessary to optimize doping methods, improve linear response at extreme doses, and develop new approaches to signal stabilization.

4.3. LiF in lithium-ion technologies

After the 1990s, the rapid development of technologies, accompanied by the widespread adoption of mobile phones, portable gadgets, and other electronic devices, became a significant driver for the intensification of research in the field of lithium-ion technologies. The continuously growing demand for compact, energy-efficient, and durable power sources prompted the scientific community to search for new materials and improve existing battery technologies.

LIBs proved to be the ideal solution to meet the requirements of modern portable devices due to their high energy density, long lifespan, and fast rechargeability. During this period, the number of scientific publications focused on improving the characteristics of LIBs surged, including research on new cathode and anode materials, electrolyte enhancements, and the development of more efficient battery management systems.

Particular attention was paid to improving the stability and safety of lithium-ion technologies. New issues and tasks emerged, focused on studying the interaction between electrodes and electrolytes, minimizing thermal risks associated with short circuits, and preventing

Table 4
Materials for thermoluminescent dosimeters (TLDs) and their main characteristics.

Material	Dopants	Radiation Sensitivity	Primary Application
LiF (Lithium Fluoride)	LiF:Mg,Ti (TLD−100)	α, β, λ, η	Universal dosimetry (medicine, ecology, personal)
	LiF:Mg,Ti (TLD−700)	α, β, λ (enriched 7Li)	Dosimetry in conditions with no significant neutron radiation
	LiF:Mg,Ti (TLD−600)	η (enriched 6Li)	Neutron dosimetry in nuclear energy and reactor environments
	LiF:Mg,Cu,P (TLD-700H)	α, β, λ (very high sensitivity)	Low doses in medical and personal dosimetry
	LiF:Mg,Cu,P (TLD-100H)	α, β, λ, η	Low-dose dosimetry in neutron irradiation conditions
$CaSO_4$ (Calcium Sulfate)	$CaSO_4$:Dy (TLD−900)	α, β, λ	Narrow dose ranges, high-sensitivity personal dosimetry
	$CaSO_4$:Eu	α, β, λ	Radiation protection
CaF_2 (Calcium Fluoride)	CaF_2:Dy (TLD−200)	α, β, λ	Medical and industrial applications
	CaF_2:Mn (TLD−300)	α, β, λ	Radiation protection and low-dose monitoring
Al_2O_3 (Aluminum Oxide)	Al_2O_3:C (TLD−500)	α, β, λ (high sensitivity and linearity)	Medical dosimetry (radiotherapy, diagnostics)
	Al_2O_3:Mg,Y	α, β, λ	Medical and industrial dosimetry
$Li_2B_4O_7$ (Lithium Tetraborate)	$Li_2B_4O_7$:Mn	α, η	Dosimetry in weak neutron background conditions
	$Li_2B_4O_7$:Cu,In	α, η (increased sensitivity)	Personal and medical dosimetry
MgB_4O_7 (Magnesium Tetraborate)	MgB_4O_7:Dy, Eu	α, η	Universal dosimetry
$BaSO_4$ (Barium Sulfate)	$BaSO_4$:Dy	α, β, λ	Radiation protection
BaF_2 (Barium Fluoride)	BaF_2:Ce	α (high doses)	Industrial dosimetry
SiO_2 (Silicon)	SiO_2 (Glass)	α, β, λ	Long-term dose monitoring (RPLD)
Topaz ($Al_2SiO_4(F, OH)_2$)	Topaz-Teflon	α (high doses)	High-dose dosimetry
	Topaz-Glass	α (high doses)	High-dose dosimetry
ZrO_2 (Zirconium Dioxide)	ZrO_2:Eu,Sm	α, β	Low signal attenuation
Y_2O_3 (Yttrium Oxide)	Y_2O_3:Tb	α, β	Personal and medical dosimetry
Polymeric Materials	Polymers with Carbon Nanotubes	Depends on matrix and filler	Experimental dosimetry

Table 5
Types of radiation detected by lithium fluoride and their characteristics.

Type of Radiation	Characteristics	LiF Detection Features	Applications
Gamma Radiation (γ)	High-energy electromagnetic radiation with strong penetrating ability.	- High sensitivity. - Linear response in dose range from mGy to Gy.	Radiotherapy, environmental monitoring, personal dosimetry.
X-ray Radiation	Electromagnetic radiation with lower energy than γ-rays.	- Good tissue equivalence (Zeff = 8.14). - Wide dose range.	Medical diagnostics, personal dosimetry.
Beta Radiation (β)	Stream of electrons or positrons with low penetrating ability.	- Requires optimization of detector thickness for efficient absorption.	Work with radioactive isotopes, personal dosimetry.
Neutrons	Electrically neutral particles with high penetrating ability.	- Indirect detection via lithium−6 reaction (6Li + n → 3 H + 4He). - Utilizes isotopic forms of LiF.	Nuclear energy, neutron dosimetry.
Alpha Radiation (α)	Stream of helium nuclei with low penetrating ability.	- Detected only upon direct contact with the material.	Rarely used; monitoring of alpha sources.
Cosmic Radiation	High-energy particles (protons, electrons, heavy nuclei).	- Effective for detecting high-energy particles and secondary radiation.	Space research, aviation.

Table 6
Types of thermoluminescent dosimeters (TLD) based on LiF and their main characteristics.

TLD Type	Material Composition	Lithium Isotopic Composition	Radiation Sensitivity	Primary Applications
TLD−100	LiF:Mg,Ti	Natural lithium (6Li: ~7.5 %, 7Li: ~92.5 %)	Sensitive to gamma, X-ray, beta radiation, and neutrons.	Universal dosimetry (medicine, environmental monitoring, personal dosimetry).
TLD−700	LiF:Mg,Ti	Enriched 7Li (~99.9 %)	Sensitive to gamma, X-ray, and beta radiation. Not sensitive to neutrons.	Dosimetry in environments without significant neutron radiation.
TLD−600	LiF:Mg,Ti	Enriched 6Li (~95 %)	High sensitivity to neutrons (reaction 6Li + n → 3 H + 4He).	Neutron dosimetry in nuclear power and reactor environments.
TLD-700H	LiF:Mg,Cu,P	Enriched 7Li (~99.9 %)	Extremely high sensitivity to gamma and X-ray radiation; insensitive to neutrons.	Low-dose measurements in medical and personal dosimetry.
TLD-100H	LiF:Mg,Cu,P	Natural lithium	High sensitivity to gamma, X-ray, and neutron radiation.	Low-dose dosimetry in environments with neutron exposure.
TLD-600H	LiF:Mg,Cu,P	Enriched 6Li (~95 %)	High sensitivity to neutrons.	Neutron dosimetry (nuclear physics and energy sectors).

material degradation under intensive use. The use of LiF in battery technologies helped address these challenges in the energy sector, including improving efficiency, safety, and battery longevity, which in turn supports the energy boom and the transition to more sustainable energy sources. Accordingly, this has led to an increase in research due to technological breakthroughs and stimulates funding for such technologies in different countries. Data obtained from Scopus shows that the number of publications, by country and by affiliation, continues to increase (Figs. 11 and 12). From these two figures, you can see the distribution of the number of publications devoted to research on LiF

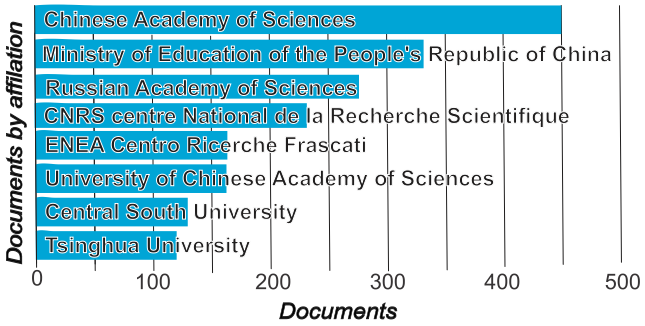

Fig. 11. Number of publications, by affiliation, over the entire period of time devoted to the study of LiF crystals.

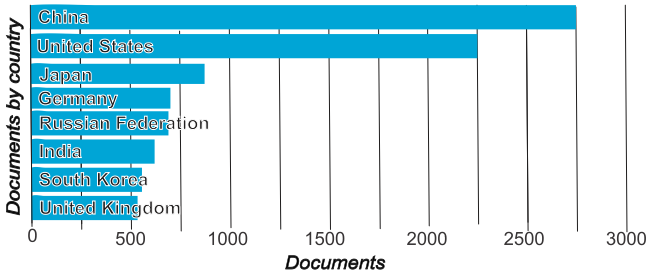

Fig. 12. Number of publications, by country, over the entire period of time devoted to the study of LiF crystals.

crystals, across 10 countries and by affiliation for all time and for the last 10 years.

From the information presented in the graph, it is worth noting that:

China: Approximately 2700 publications, which is the largest number among all countries.

USA: Approximately 2400 publications, ranked second, and so on. It can be seen that China and the USA are leaders in LiF crystal research, each with 2000 + publications. Japan, Germany, and the Russian Federation follow in the next positions in terms of the number of publications, indicating their active engagement in this area of research. Of course, this is a rough visual representation of the data. But overall (without considering the quality or impact of each publication), the graph provides a valuable overview of global activity in the field of LiF crystal research.

Recently, research has become increasingly interdisciplinary, combining fields such as physics, chemistry, materials science, and engineering (Fig. 13). The number of publications devoted to LiF surface research [50,51] continues to grow. New research methods, such as computer modeling [52,53] and nanotechnology, are opening up new possibilities for studying and using the LiF surface. LiF surface research

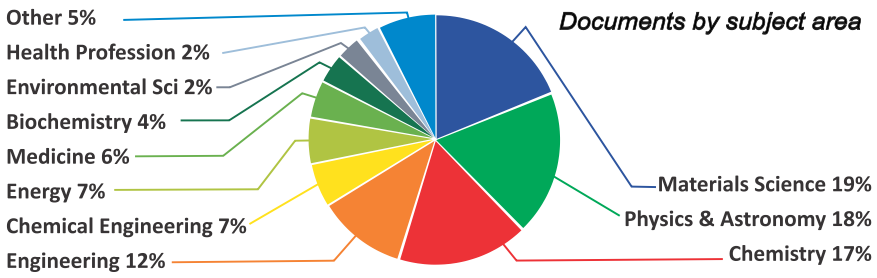

Fig. 13. Number of publications by scientific field for the entire time devoted to the study of LiF crystals.

is of great importance for the development of new technologies and the improvement of existing lithium production [54,55].

Fig. 13 shows the distribution of publications in the form of a pie chart on LiF crystal research as a percentage of the total number of publications in various scientific fields.

Several important conclusions can be drawn from the diagram:

The dominant areas of research are materials science (19.1 %), physics (18.3 %), and chemistry (17.6 %), collectively accounting for about 55 % of all publications. This highlights the significance of LiF in both fundamental and applied research across materials, physics, and chemistry. Engineering applications (12.1 %) and chemical engineering (6.9 %) also show a substantial number of publications. The proportion dedicated to energy applications (6.7 %) underscores LiF's importance in fields like batteries [56,57] and nuclear technologies [58,59], aligning with contemporary trends in renewable energy sources and energy storage.

The remaining publications cover biomedical and environmental research, including medicine (5.5 %), biochemistry, genetics, and molecular biology (3.8 %), environmental sciences (2.5 %), and health professions (2.4 %). This diversity illustrates the wide-ranging applications of LiF beyond the fields mentioned above.

From Fig.s 4 and 13, it is evident that lithium fluoride has been actively utilized in recent years for electrochemistry and energy applications as an electrolyte in solid-state LIBs [60]. The development of LIBs has enabled significant progress in portable electronic devices and facilitated the integration of electric vehicles. However, the low potential of anode reactivity necessitates the formation of a solid electrolyte interface (SEI) to passivate the electrode surface and ensure long-term cycling stability. Despite decades of research on SEI, a comprehensive understanding of its formation mechanisms and evolution remains elusive. The instability of SEI components leads to their decomposition, resulting in gas formation [61] and solute species in the electrolyte. This evolution increases SEI porosity, further electrolyte reduction, and thickening of SEI layers. Developing more stable SEI components is crucial for enhancing battery performance. Let us briefly examine the concept of SEI and its characteristics.

The SEI is a solid electrolyte interphase film that forms on the surface of the anode in rechargeable lithium batteries (such as lithium-ion or lithium-metal batteries) [62]. It is created as a result of chemical reactions between the electrolyte and the anode material during the initial charging of the battery.

The primary function of the SEI is to protect the anode. Acting as a barrier, it allows only lithium ions (Li^+) to pass through while blocking the movement of electrons. The SEI prevents further decomposition of the electrolyte on the anode surface by forming a protective layer. This enables the battery to operate over many charge/discharge cycles, thereby extending its lifespan. Additionally, the SEI helps mitigate the growth of lithium dendrites, which can cause short circuits and reduce the battery's safety.

As shown in Table 7, the SEI consists of two main layers:

1. **Inner Layer (Inorganic):**
   - Located closer to the anode.
   - Key components: LiF, Li_2O, Li_2CO_3, Li_3N, LiOH.
   - Dense and compact, responsible for protecting the anode.
2. **Outer Layer (Organic):**
   - Positioned closer to the electrolyte.
   - Key components: organic electrolyte decomposition products (e.g., polymers or carbonates).
   - Porous, facilitating lithium-ion penetration.

Table 7
Key compounds in SEI.

Compound		Characteristics	Percentage in LIB
Inorganic	**Lithium Fluoride (LiF)**	High chemical stability. Low ionic conductivity.	20–30 %
	Lithium Carbonate (Li_2CO_3)	Provides mechanical stability. Prevents dendrite growth.	30–40 %
	Lithium Oxide (Li_2O)	Forms a dense layer. Protects the anode from reactions with the electrolyte.	10–15 %
	Lithium Nitride (Li_3N)	High ionic conductivity. Stabilizes the anode.	< 5 %
	Lithium Hydroxide (LiOH)	Less stable. May contribute to SEI degradation.	< 5 %
Organic	**Lithium Fluoride (LiF)**	Form a porous outer layer. May be less stable.	20–25 %
	Lithium Alkylcarbonates	Provide flexibility to SEI. Reduce side reactions.	5–10 %
	Polymers	Enhance SEI stability. Reduce ionic conductivity.	< 5 %
	Lithium Silicate ($LixSiO_y$)	Forms on silicon anodes. Stabilizes SEI on Si.	Depends on the anode (up to 30 % on Si)

The percentage composition in LIBs varies depending on the electrolyte composition and the type of anode (e.g., graphite, silicon, or lithium metal). As indicated in Table 7, the most prevalent SEI components are LiF and Li_2CO_3, owing to their stability and protective properties. Organic compounds are more commonly found in the outer layer, which interacts directly with the electrolyte. A deeper understanding of the nanostructure of SEI components and ionic transport along particle grain boundaries is critical for advancing this field. Additionally, a better understanding of the nanostructure of SEI components and ion transport along grain boundaries is critically important for advancing in this direction. Of course, LiF has not been left out in this regard. In Fig. 14-a, you can observe the mechanism and composition of the initial SEI [63]. As you can see, LiF is utilized as part of the SEI.

Based on these initial results, an approximately 50 nm thick SEI composed of lithium ethylene dicarbonate and LiF is generated, which can function as an effective passivation layer, thereby preventing further electrolyte decomposition and graphite peeling, as shown in Figs. 14-b and 15.

As it can be seen, at this stage of development, LiF is actively used as

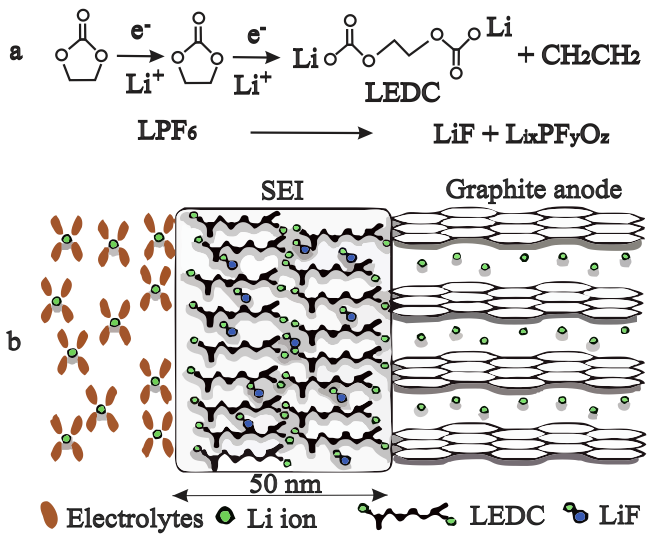

Fig. 14. Formation mechanism and composition of initial SEI. (a) Initial ethylene carbonate reduction reactions at the interface of graphite electrodes. (b) Schematic representation of the initial SEI formed on the graphite surface during the first cycle of operation of a Li-ion battery. Reproduced from [63] with permission.

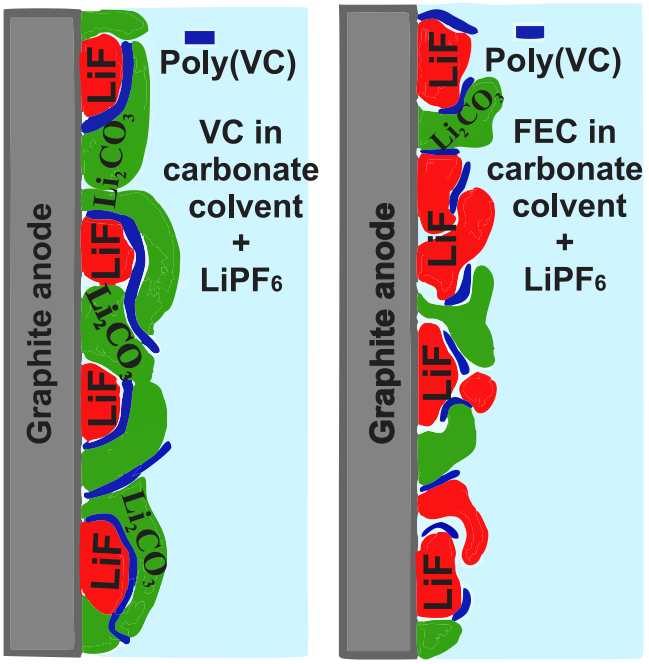

Fig. 15. Schematic representations of the initial SEI generated on graphite anodes for electrolytes containing vinylene carbonate (left) or fluoroethylene carbonate (right). Reproduced from [64] with permission.

SEI. While not a primary material in traditional LIBs, it finds application in various auxiliary and innovative contexts related to lithium-ion technologies [65]. Lithium fluoride is sometimes used as a component in electrolytes to stabilize and enhance their characteristics [66,67]. It can help mitigate electrolyte decomposition [68] and improve battery performance at high voltages [69,70]. Introducing LiF into the electrolyte can also enhance thermal stability and safety [71,72]. In solid-state lithium-ion battery research and development, LiF can be used as part of composite materials for solid electrolytes. Solid electrolytes have the potential to significantly increase safety and energy density compared to traditional liquid electrolytes [73,74]. Lithium fluoride may be present in the SEI layer on the anode surface. The SEI layer forms during initial charge/discharge cycles and plays a crucial role in protecting the anode and ensuring battery stability. LiF can contribute to improving the stability of the SEI layer, thereby enhancing battery durability and performance.

Lithium fluoride can also be used as an additive in cathode materials to improve their structural stability and cyclic longevity. This is particularly important for cathodes operating at high voltages, where material stability is critical to prevent degradation [75–77]. Recent studies have shown [78] that adding LiF to various components of LIBs can significantly enhance their performance. For instance, research indicates that a small amount of LiF [79] added to the electrolyte can enhance cathode stability and reduce degradation rates over multiple charge-discharge cycles. Also, in study [80], the authors used LiF in phosphorus-based batteries. The research showed that LiF plays a key role in addressing the issue of soluble potassium polyphosphates encountered when using phosphorus as an anode material for potassium-ion batteries. LiF prevents the penetration of polyphosphates into the electrolyte before and after the formation of the SEI and, in combination with replacing the electrolyte KPF_6 with KFSI, promotes the formation of a thin, stable, and homogeneous SEI layer on the electrode particle surface. Thanks to LiF, the initial coulombic efficiency increases to 73.7 %, and the reversible specific capacity reaches 507.6 mAh•g-1 after 100 cycles at a current of 50 mA•g-1. Overall, LiF helps address the issue of soluble potassium polyphosphates, leading to improved initial efficiency, capacity, and cyclic stability of phosphorus-based potassium-ion battery systems.

In this [78] study, the authors propose using a composite protective layer LiF-Li_3N, which forms in situ on the surface of the lithium anode. LiF-Li_3N possesses high interfacial energy and adhesion, allowing it to effectively suppress side reactions and inhibit lithium dendrite growth. Fig. 16 from this study demonstrates the impact of the LiF-Li_3N protective layer on the cyclic capacity and stability of solid-state lithium batteries with a $LiCoO_2$ cathode.

From Fig. 16, it can be seen that the fabricated LiF-Li_3N protective layer in solid-state lithium batteries prevents side reactions between lithium and the sulfide solid electrolyte, improves the reversibility of lithium stripping/plating, thereby suppressing lithium dendrite formation. Thanks to the LiF-Li_3N protective layer, the critical current densities of Li@LiF-Li_3N cells with $Li_{10}GeP_2S_{12}$ and Li_6PS_5Cl electrolytes can reach high values of 3.25 and 1.25 mA·cm−2, respectively. As a result, the batteries demonstrate excellent cyclic stability over 500 cycles with capacity retention of 93.5 % and 89.2 % at 1 C charge or discharge rate, respectively.

Comparing these studies, in both cases LiF enhances battery performance, but through different mechanisms. In the first study, LiF acts as a barrier, preventing the negative impact of soluble components on the electrolyte, whereas in the second study, LiF is part of a protective layer that directly interacts with the lithium anode, stabilizing its surface.

Overall, LiF demonstrates its versatility and effectiveness in addressing various challenges in solid-state batteries. Its use contributes to the development of solid-state batteries, enhancing their safety, performance, and longevity. Below, we will delve into some studies that feature existing and new technologies, ultimately leading to the transition to solid-state batteries.

The study [79] investigates the use of mesoporous $LaxCoO_{3-\delta}$ nanofibers with controlled cationic defects as a composite polymer-oxide electrolyte component for all-solid-state lithium-metal batteries. The main goal of the work was to address the challenge of managing interactions between components in such electrolytes to enable efficient Li^+ ion transport and stable interfacial contact between the CPE and the electrode. To achieve this, the authors proposed using $LaxCoO_{3-\delta}$ nanofibers with a controlled level of cationic defects at the A-site (La), with x ranging from 1.0 to 0.8, which enhanced the interaction between the nanofibers and the PEO/LiTFSI polymer electrolyte.

In addition, the study highlights the importance of the LiF/Li_3N

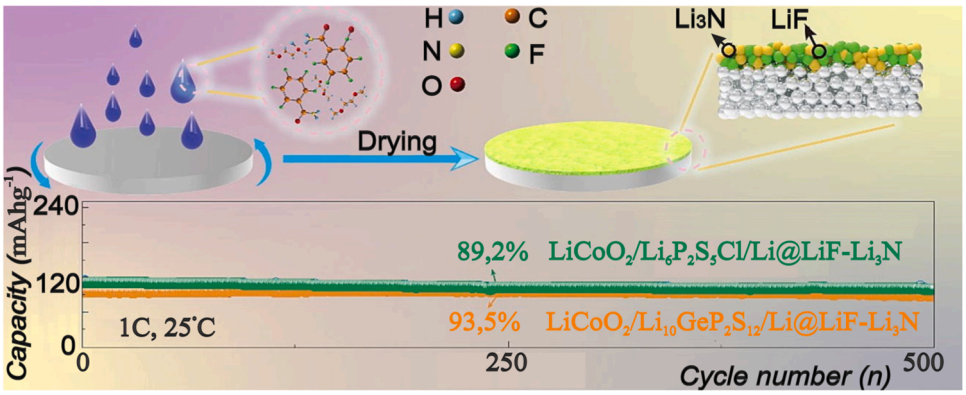

Fig. 16. Effect of LiF-Li_3N protective layer on the cycling capacity and stability of solid-state lithium batteries with $LiCoO_2$ cathode. Reproduced from [78] with permission.

interfacial layer, which facilitates high ionic conductivity and ensures high electrochemical stability of the system. The combined use of $La_xCoO_{3-\delta}$ nanofibers and the LiF/Li_3N interfacial layer significantly improves the performance of solid-state lithium-metal batteries, including enhanced interfacial stability, reduced dendrite growth risk, and extended operational lifespan.

The problem of an unstable electrolyte/electrode interface, with dendrite growth and increased resistance, significantly reduces the safety and efficiency of all-solid-state lithium-metal batteries. In the study [81] an "in situ LiF nanodecoration" method is proposed to address this issue. The approach involves the uniform distribution of ultrathin LiF nanoparticles in an amorphous $Li_2B_{12}H_{12}$ matrix, which is formed in situ through a solid-phase reaction.

Characteristics of the new composite electrolyte:

- Li-ion conductivity: 5×10^{-4} S/cm at 75°C.
- Low electronic conductivity: 9×10^{-1} ° S/cm at 75°C.
- High compatibility with the electrode due to the formation of stable electrolyte/electrode interfaces.
- Dendrite suppression capability: critical current density of 3.6 mA/cm^2.
- Low interfacial resistance: 746 Ω·cm^2 after 10 cycles at 75°C.

The new composite electrolyte contributes to the stable cycling of Li-$LiFePO_4$ ASSB, paving the way for the use of in situ nanodecoration chemistry to develop safe and highly efficient batteries.

The issue of low lithium-ion conductivity at room temperature is a significant challenge for polymer electrolytes, although polymer solid electrolytes possess flexibility and high safety.

In the study [82], polymer-ceramic composite electrolytes were developed for high-energy solid-state lithium-sulfur (Li-S) batteries. Specifically, the use of a flexible composite polymer-ceramic electrolyte, consisting of polyvinylidene fluoride and garnet-type $Li_{6.5}La_{2.5}Ba_{0.5}ZrTaO_{12}$, is discussed for operation at room temperature, demonstrating high lithium-ion conductivity (0.34 mS/cm at 20°C). For the first time, polyvinylidene fluoride-garnet polymer-ceramic composite electrolytes were modified with the addition of LiF, which was confirmed by stable galvanostatic cycling at 0.2 mA/cm^2 for over 800 hours. The addition of LiF improves the stability of polyvinylidene fluoride-based polymer-ceramic composite electrolytes, as confirmed by X-ray photoelectron spectroscopy and electrochemical measurements. The solid-state lithium-sulfur battery created with the modified polymer-ceramic composite electrolyte demonstrates a high specific capacity (936 mAh/g at 0.1 C and 20°C) and stable operation for over 80 cycles, as well as excellent rate capability and high efficiency. As can be seen, LiF improves the stability of these electrolytes by preventing dehydrofluorination and ensuring stable galvanostatic cycling. This significantly enhances the lifespan and efficiency of solid-state lithium-sulfur batteries at room temperature.

By 2024, a process for creating an ultrathin (200 nm) lithium fluoride coating on the surface of lithium metal using vacuum evaporation has been developed. The study [66] investigated a simple and controlled surface fluorination method to create a dense and uniform ultrathin protective LiF coating on the surface of lithium metal via vacuum evaporation. As a result, dendrite-free deposition was achieved at a high current density of 3 mA/cm^2. Full cells, LiF@Li|$LiFePO_4$, with *a* LiF-coated anode (200 nm thick), demonstrated up to 85.31 % capacity retention over 600 cycles. Stable lithium deposition was achieved for 1200 hours under limited electrolyte conditions. The conclusion was made that the protective lithium fluoride coating is a promising approach for enhancing the stability and safety of lithium-metal anodes. This method allows for the creation of stable interfaces and improved lithium-ion conductivity, leading to improved cycling stability and overall battery performance.

The studies [83,84] focus on the role of lithium fluoride in the composition of the SEI. These works highlight the fundamental aspects, characteristics, and potential applications of LiF in lithium-based batteries. LiF, as an inorganic component of SEI, contributes to the uniform distribution of lithium-ion (Li^+) fluxes and minimizes undesirable reactions between the anode and the electrolyte. However, the exact mechanism of Li^+ transport through the SEI remains insufficiently understood. It is hypothesized that LiF forms dense nanostructures, enabling Li^+ transport along grain boundaries. While LiF is often regarded as a critical protective component of SEI, some studies [85,86] suggest that its role is limited and that it does not always form a dense layer in contact with the electrolyte. Despite these disagreements, understanding SEI processes remains crucial for the development of batteries with high energy density, durability, and safety. LiF remains a central focus in this field due to its protective properties and stability.

High-voltage lithium batteries, as discussed in [87,88], represent the next stage in lithium battery evolution. They aim to enhance energy density, longevity, and safety. A key factor in their performance is the stability of the SEI and the cathode electrolyte interphase, where LiF plays a significant role.

Additionally, the development of new solid polymer electrolytes [89,90] offers significant potential for advancing energy storage technologies. In such systems, LiF remains an important component, ensuring interface stabilization and extending battery life [91,92].

In conclusion, LiF continues to be a critical element in research on next-generation lithium batteries, contributing to their stability, durability, and performance enhancements.

Thus, LiF exhibits high electrochemical stability, especially under high voltage conditions, making it an ideal material for protecting the interface between the anode (typically lithium metal or graphite) and the electrolyte. This helps reduce lithium dissolution and the formation of a more stable and durable SEI. SEI is a key component in LIBs that

prevents further reactions between the anode and the electrolyte. However, the SEI can become unstable during prolonged cycling, leading to battery degradation. LiF helps stabilize this layer, making it more resistant to decomposition, and also reduces the formation of by-products such as lithium salts and gaseous products. Additionally, LiF has high thermodynamic stability and does not react with the electrolyte at high temperatures, which helps maintain the long-term integrity of the SEI interface and improves the cyclic stability of the battery.

Furthermore, LiF can also act as a mechanical stabilizer, as fluorides such as LiF have high hardness and resistance to chemical and mechanical damage. This can help strengthen the SEI structure, especially under mechanical stresses that may arise during battery cycling (e.g., during expansion and contraction of the anode material). The incorporation of LiF into the SEI improves the homogeneity of the interface, which helps reduce material degradation and extends the battery's lifespan.

The advantages of LiF in LIBs lie in its ability to stabilize the anode surface, preventing lithium dissolution and minimizing the formation of by-products in the electrolyte. Such a layer helps reduce gas formation, which may result from reactions with the electrolyte. This is important for preventing an increase in pressure within the battery and maintaining safe operation. In conclusion, it can be confidently stated that the stabilization of the SEI with LiF is the result of both electrochemical and mechanical factors. Primarily, LiF acts as an electrochemical stabilizer, enhancing the stability of the interface and reducing side reactions, which directly impacts the long-term performance of the battery. Mechanical factors include the improvement of the strength and resistance of the SEI to physical and chemical changes, which also contributes to its longevity. However, new methods and approaches are required to understand the molecular mechanisms underlying SEI formation and the role of LiF during charge/discharge cycles. Special attention should be given to the development of artificial interphase films with an optimal LiF content. Ultimately, many studies [93–97] indicate that the transition to solid-state batteries is inevitable, with LiF playing a significant role.

4.4. Application of LiF in nuclear technologies

Nuclear energy is one of the key sources of energy for ensuring the stability of energy systems in developed countries [98]. It helps minimize dependence on fossil fuels, reduce greenhouse gas emissions, and ensure long-term energy security [99].

After the introduction of nuclear reactors in the 1950s, one of the key scientific and technical challenges became ensuring effective cooling of their active zones. The creation of a high-quality heat transfer system in the active zone of nuclear reactors is necessary to ensure efficient heat removal generated during nuclear reactions [100]. Effective heat transfer improves the operational performance of the reactor [101], enhances its safety, and extends the service life of structural components [102]. This challenge became a key element in the design of nuclear reactors [103]. After a thorough analysis of numerous reviews and scientific papers in this field, we have compiled the following tables. Nuclear reactors are categorized into generations based on their technological level [104], safety [105], efficiency, and stability [106]. Table 8 presents their main characteristics.

As seen, generation IV reactors represent the future of nuclear energy. The main focus here is on a closed fuel cycle and minimizing waste. These reactors include Molten Salt Reactors (MSR), Sodium-cooled Fast Reactors (SFR), and Very High Temperature Reactors (VHTR).

In the next Table 9, a comparison of nuclear reactors based on their years of operation, current use, and development status is presented.

The Table 9 shows that the Light Water Reactor (LWR) is the most widespread type of reactor in the world, with over 400 units. The first commercial LWRs began operation in the 1960s and are used in nuclear power plants in many countries, including the USA, France, Russia, China, and others. The first developments of Sodium-cooled Fast Reactors (SFR) began in the 1960s (e.g., the Phenix reactor), but these reactors faced issues due to the chemical activity of sodium. Today, more advanced versions, such as Natrium, are actively being developed. The first experimental SFR was EBR-I (USA, 1951). Russia actively operates the BN-600 and BN-800, with the BN-1200 project in preparation. Prospects are associated with a closed fuel cycle and the use of reprocessed fuel.

Lead-cooled Fast Reactors (LFR) appeared in the 1990s but remain in the development stage as part of Generation IV technologies, with examples such as the MYRRHA project. Their appeal lies in corrosion resistance and radioactive safety. Currently, only prototypes exist, such as the Russian "Brest-OD-300" project.

Supercritical Water Reactors (SCWR) are still under development because supercritical water requires complex materials to operate under extreme conditions. The main advantage is high thermal efficiency.

Molten Salt Reactor (MSR): The first prototypes (MSRE in the USA) were developed in the 1960s, but commercial operation never began.

Table 9
Comparison of nuclear reactors by years of operation, current use, and development status.

Reactor Type	Combined Information	Current Status
Light Water Reactor (LWR)	1950s, Water (H_2O), ~300°C	Widely used (AP1000, etc.)
Sodium-cooled Fast Reactor (SFR)	1960s, Liquid Sodium, ~550°C	In use, new projects under development (e.g., BN−800, Natrium)
Lead-cooled Fast Reactor (LFR)	1990s (design), Liquid Lead or Lead-Bismuth Alloy, ~500°C	Compact, promising development (MYRRHA)
Supercritical Water Reactor (SCWR)	2000s (design), Supercritical Water, ~600°C	Under development
Molten Salt Reactor (MSR)	1960s (design), Fluoride Salts, ~700°C	Promising development for small modular reactors (ThorCon, Terrestrial Energy IMSR)
Fluoride Salt Reactor (FHR)	2010s, Fluoride Salts, ~850°C	Under development (FuSTAR, AHTR)
Gas-cooled Fast Reactor (GFR)	2000s (design), Gas (Helium or Carbon Dioxide), ~900°C	Under development, promising project within Gen IV
Very High Temperature Reactor (VHTR)	1970s, Helium, > 900°C	Promising project for hydrogen energy (HTR-PM, Xe−100)
Heavy Metal Fast Reactor (HTMR)	1990s, Lead, Bismuth, ~500–600°C	Promising project

Table 8
Comparison of nuclear reactor generations.

Parameter	Generation I	Generation II	Generation III	Generation III+	Generation IV
Development period	1950s–1960s	1970s–1990s	1990s–2000s	2000s–present	Expected after 2030
Examples of reactors	Magnox, AMB	PWR, BWR, CANDU, VVER	EPR, AP1000, VVER−1200	Hualong One, APR1400	MSR, SFR, SCWR, VHTR
Coolant types	Gas, water	Water	Water	Water	Sodium, lead, helium, molten salts
Coolant temperature	~250–300°C	~300°C	~300°C	~300°C	500–1000°C
Efficiency	~25 %	~30–33 %	~35 %	~37 %	~45–50 %
Service life	20–30 years	30–40 years	40–60 years	60 + years	60 + years

Today, promising variants are being developed. The first experimental reactor operated in the USA (ORNL, 1965–1969). MSRs are not in use due to challenges with fuel reprocessing, but their prospects have revived with the development of small modular reactors [107].

Fluoride Salt Reactors (FHR): This is a new generation of reactors based on the success of MSRs but with improved coolants. Examples include AHTR and FuSTAR. It is a more modern concept, related to MSRs but using graphite moderators and solid fuel. Currently, it is under investigation and is considered for hydrogen production and space applications [108].

Gas-cooled Fast Reactors (GFR) and Very High Temperature Reactors (VHTR) emerged later, as they require complex technologies and materials [109]. They attract attention due to their high outlet temperatures and potential for hydrogen production. The concept was explored in the 1960s and 1970s but was not realized due to material challenges. Prospects are linked to operation at high temperatures and resistance to accidents. The VHTR (Very High Temperature Reactor) experiments began in the 1970s (e.g., the AVR project in Germany) and are used on a limited scale, such as in China.

As follows from the information in Table 9, one of the key tasks in the design of nuclear reactors is ensuring efficient heat transfer. For this, a material is required that possesses high thermal conductivity, resistance to extreme temperatures, radiation resistance, corrosion resistance, and meets safety requirements. The high radiation and extreme temperature resistance of LiF makes it an ideal material for operation in the harsh conditions typical of nuclear energy. One of its key applications is in the composition of flux salts for nuclear reactors, such as MSRs [110].

The first work on MSR was in 1954 [111], on an experimental aircraft with a molten fuel reactor and a coolant consisting of molten fluoride salts, which was tested for 100 hours of operation. The second was a civilian power plant based on MSR [112]. However, for some reasons, this experimental project was rejected by the government. The working principle of MSR is shown in Fig. 17.

To date, pure LiF is not used in MSR reactors due to its limited properties, which do not fully meet the needs of the reactor environment. Instead, multi-component mixtures based on LiF are used. For example, a study [113] focuses on the properties and structure of molten salts used in nuclear technologies, with an emphasis on actinide-containing compounds such as fluorides and chlorides. Lithium fluoride is mentioned in the context of MSRs, where it is used in multi-component fuel salt mixtures, such as LiF-ThF_4-UF_4-PuF_3.

It is shown that LiF is a key component in MSRs due to its high thermal stability, low viscosity, and low neutron capture cross-section. Additionally, in mixtures with other fluorides (such as ThF_4 and UF_4), LiF helps create a stable liquid structure that enables efficient heat transfer and the removal of fission products. It is emphasized that mixtures like LiF-ThF_4 have a complex structure involving polyhedral complexes ($[ThF_8]^{4-}$) that form networks with various atomic coordination.

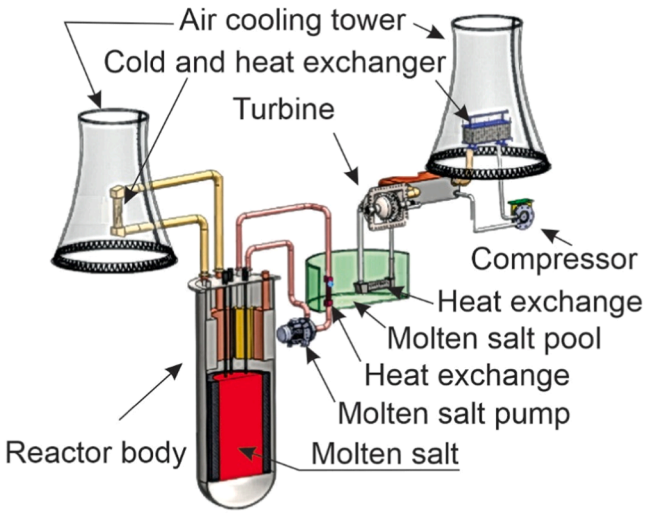

Fig. 17. Operating principle of a MSR with LiF.

The study [114] analyzes the Fluoride-Salt-cooled high-Temperature Advanced Reactor (FuSTAR) — a compact fourth-generation nuclear reactor. The reactor uses fluoride salts such as LiF-BeF2 (FLiBe) as a coolant, providing high thermal conductivity, corrosion resistance, operation at atmospheric pressure, and temperatures up to 700°C. The reactor employs the supercritical Brayton cycle with CO2, achieving thermal efficiency of up to 53 %. The reactor is designed to operate at high temperatures (up to 700°C), enabling its use in thermochemical hydrogen production, oil refining, desalination, and other industrial processes. Emergency scenarios, such as loss of cooling, are considered, showing that the system remains stable. The challenges of tritium generation and management to reduce its environmental impact are discussed. It is demonstrated that FuSTAR offers high economic efficiency, safety, and broad application potential, including the transition to carbon-free energy. Lithium fluoride in reactors such as the FuSTAR has advantages that distinguish it from other types of reactors [115–118]. Thus, FuSTAR achieves the highest thermal efficiency (53 %) due to the use of fluoride salts and the supercritical Brayton cycle. These reactors have varying levels of maturity and are aimed at unique tasks—from decarbonization to industrial heat utilization. FuSTAR and AHTR are ideal for countries striving for a carbon-free economy. They can replace fossil fuels in electricity and heat production. Additionally, they are perfectly suited for thermochemical hydrogen production, oil refining, chemical production, and desalination. Modular reactors like FuSTAR can be used in remote or isolated regions where developing a centralized energy grid is challenging. The AP1000 will continue to be used for large-scale electricity production in centralized energy systems. Fast reactors (Phenix, SFR) will help close the fuel cycle, minimize waste, and recycle actinides.

This figure demonstrates the temperature range of the coolant at the outlet from the active zone of various types of nuclear reactors and their potential applications in different industrial processes. Each type of reactor has its own area of application. Fluoride salt reactors represent the future of the hydrogen economy and industrial heat, AP1000 remains key for large-scale electricity generation, and fast reactors like Phenix are used for closing the fuel cycle.

LiF-based reactors provide a unique combination of safety, thermal efficiency, and durability. Unlike other types of reactors, the use of LiF allows operation at higher temperatures without high pressure, reduces corrosion effects and leakage risks, and enhances neutron safety due to its low capture cross-section. These properties make LiF-based reactors more competitive and promising for use in modern energy, industry, and space applications. However, the future of nuclear energy is not stagnant; it is evolving with the adoption of intelligent systems [103,119], innovative materials, and advanced modeling-based programs [120]. These advancements enable the development of more efficient reactor designs [121], the enhancement of safety systems, and improvements in nuclear waste management. Cutting-edge modeling technologies and artificial intelligence allow for highly accurate predictions of reactor behavior, fuel optimization, and reduced environmental impact [122]. Additionally, the application of new materials [123], such as accident-tolerant fuels and advanced composites, contributes to increased reactor efficiency and longevity. These innovations pave the way for the next generation of nuclear technologies that promise to be more sustainable, cost-effective, and safer.

4.5. Application of LiF in PLED and OLED Cathodes

This section discusses the key aspects of LiF application in PLED and OLED cathodes, including its impact on electron emission, mechanisms for improving electron injection, and recent advancements in this field.

The development of display technologies has gone through several key stages, from cathode ray tubes (CRT) to modern organic light-emitting diodes (OLED) [124] and their advanced versions, AMOLED [125,126]. Each generation of displays has brought significant improvements in characteristics such as image quality, energy consumption, screen thickness, and response speed.

The simplest energy scheme of the OLED matrix operation principle is shown in Fig. 19. The figure illustrates the process of electron and hole recombination in OLED displays. It demonstrates the process where, under the influence of an electric field, electrons from the cathode and holes from the anode move towards the active layer. In the active layer, they recombine, resulting in the emission of light (photons). This process forms the basis for the operation of OLEDs, used in displays to create bright and energy-efficient images.

ITO (anode) — Indium Tin Oxide, used as a transparent electrode. HTL — Hole Transport Layer, ensures hole transport to the emissive layer. EBL — Electron Blocking Layer, prevents electron transfer to the anode. EML — Emissive Layer, where electron-hole recombination occurs, leading to light emission. HBL — Hole Blocking Layer, prevents hole transfer to the cathode. ETL — Electron Transport Layer, helps direct electrons to the emissive layer. Substrate — The base on which all OLED layers are assembled.

Lithium fluoride also plays an important role in the development of modern organic light-emitting devices, such as OLEDs and polymer light-emitting diodes (PLED). Due to its unique properties, including high thermal stability, chemical inertness, and the ability to form interfacial layers with metals, LiF has become a key component in improving the efficiency and longevity of these devices.

The main function of LiF in the cathodes of PLED and OLED is to reduce the electron work function of the metals used as cathodes, such as aluminum. This promotes more efficient electron injection from the cathode into the device's active layer, leading to a significant increase in brightness, efficiency, and emission stability.

Recent studies show that thin LiF layers, just a few nanometers thick, applied between the cathode and the emissive layer, can significantly improve device performance by forming an ultra-thin barrier layer and enhancing the contact between the layers. These advancements have made LiF an important material in the production of displays, lighting, and other optoelectronic systems based on PLED and OLED technologies.

The use of LiF in OLEDs began with the active development of this technology in the early 2000s, when its important role in improving the performance of cathodes was recognized. LiF was applied in ultra-thin interfacial layers between the cathode (e.g., aluminum) and the

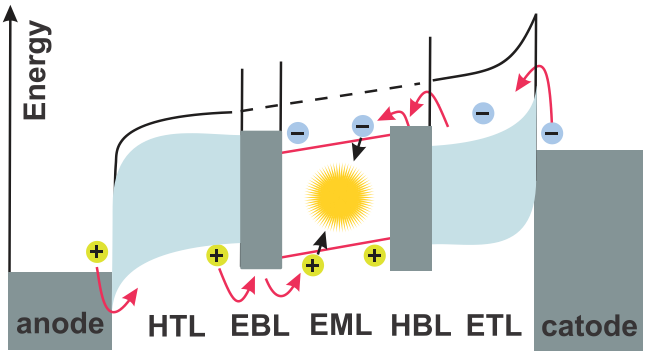

Fig. 19. The simplest energy scheme of the OLED matrix operation principle: recombination and light emission processes.

organic emissive layer. Fig. 20 shows the operating principle of OLED displays: recombination processes (a), matrix structure (b), and their applications (c).

Currently, OLED consists of a multilayered device where light emission occurs due to the recombination of electrons and holes in the emissive layer. In Fig. 20a, you can see the simplest structure of a typical three-layer OLED device. The base of the OLED is a glass substrate that provides mechanical support and transparency for light output. On top of it, an anode with a high work function is deposited: typically made from transparent conductive material, most often indium tin oxide (ITO), which is connected to the positive potential and generates holes in the organic layer.

A hole transport layer is formed between the organic layer and the anode. This layer consists of materials with high hole mobility, high glass transition temperature, and the ability to block electrons. The hole transport layer reduces the barrier for hole injection into the OLED device, facilitating their movement into the emissive layer. Copper phthalocyanine (CuPc) and m-MTDATA are commonly used materials for the hole transport layer (HTL), as their highest occupied molecular orbital (HOMO) aligns with the work function of the ITO anode, improving hole injection efficiency.

The emissive layer consists of materials with high efficiency, long lifespan, and high color purity. The main classes of materials used in the emissive layer of OLEDs include:

- Small molecules
- Polymers
- Conjugated dendrimers

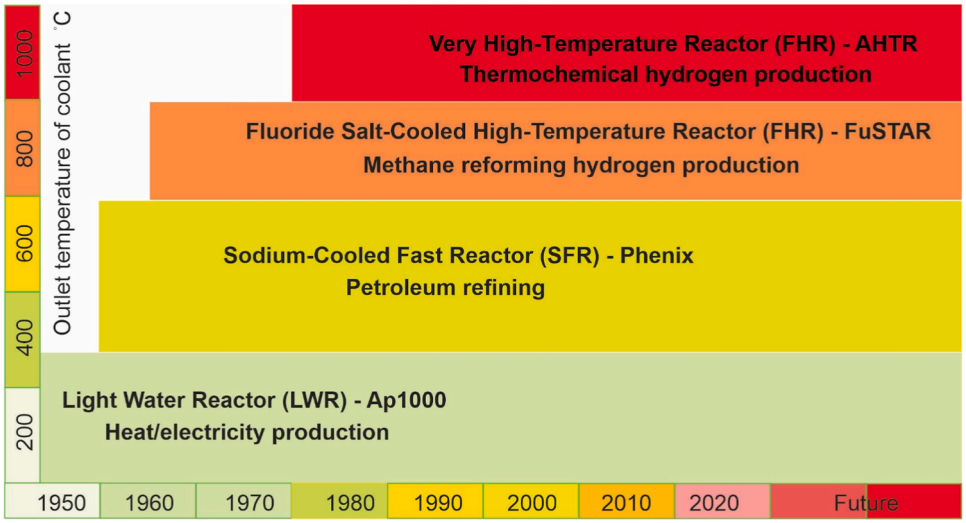

Fig. 18. Comparison of the evolution of nuclear reactors by coolant temperature and application area.

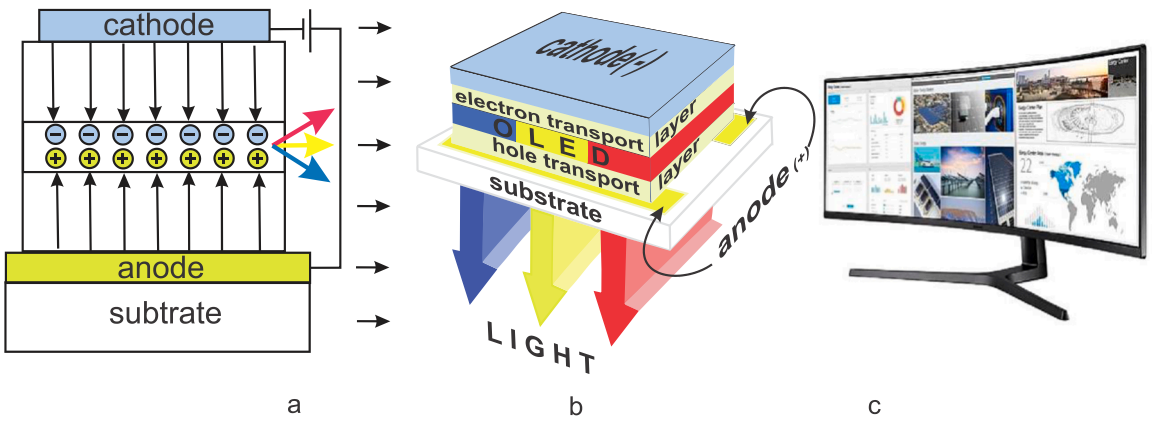

Fig. 20. Operating principle of OLED displays: recombination processes (a), matrix structure (b), and applications (c).

The emissive layer plays a crucial role in the operation of OLEDs, as it is here that the recombination of electrons and holes occurs, resulting in the emission of light. The choice of material depends on the desired color, efficiency, and lifespan of the device. The thickness of this layer typically ranges from 100 to 200 nm.

The cathode is typically made from aluminum or a metal with a low work function. It is connected to the negative potential, leading to the injection of electrons into the organic layer. A layer for electron transport is deposited between the cathode and the organic layer, which facilitates the movement of electrons from the cathode to the emissive layer. It is here that a thin layer of lithium fluoride is primarily used, acting as a barrier that facilitates electron injection.

The operating principle of this system is as follows: when a forward bias potential is applied between the anode and cathode, the anode injects positively charged holes into the hole transport layer, while the cathode injects negatively charged electrons through the electron transport layer. The thin layer of LiF facilitates the electron injection process by reducing the energy barrier. Electrons and holes move towards the emissive layer through their respective transport layers. When they meet in the emissive layer, recombination occurs, releasing energy in the form of photon emission. The light generated in the emissive layer passes through the anode and glass substrate outward.

LiF is used in the electron transport layer and plays a key role in enhancing the efficiency of OLED devices. Its main functions are to:

- Reduce the work function of electrons, making it easier to inject them into the organic layer
- Improve the stability of the cathode, preventing damage to the organic layers
- Enhance charge recombination efficiency, leading to increased brightness and reduced power consumption

Thus, the addition of LiF to the OLED structure marked an important milestone in the development of the technology, particularly for high-efficiency and durable displays.

OLED technology continues to evolve, becoming more powerful and complex. As the demands for matrices increase, such as higher frequencies, larger sizes, and other parameters, new challenges arise for developers and researchers.

In a recent study [127], optimizations were made in the structure composition of tandem OLEDs. Specifically, LiF is used as part of the charge generation layer (CGL) to improve the device's efficiency (Fig. 21a). LiF forms the LiF/Mg interface, which enhances electron injection and transport. This is part of a new approach to creating a dual-emissive layer (DEML) structure in green tandem OLEDs (Fig. 21b). It was shown that compared to previously published results, [128,129] tandem OLEDs with dual-emissive layers achieved advanced values of current efficiency up to 242.4 cd/A. Optimization of the thickness of the dual-emissive layers and resonator lengths allowed reducing the operating voltages to 4.8 and 5.4 V at different brightness levels. The devices demonstrated an extraordinarily long lifetime (LT50) of 734.8 hours at

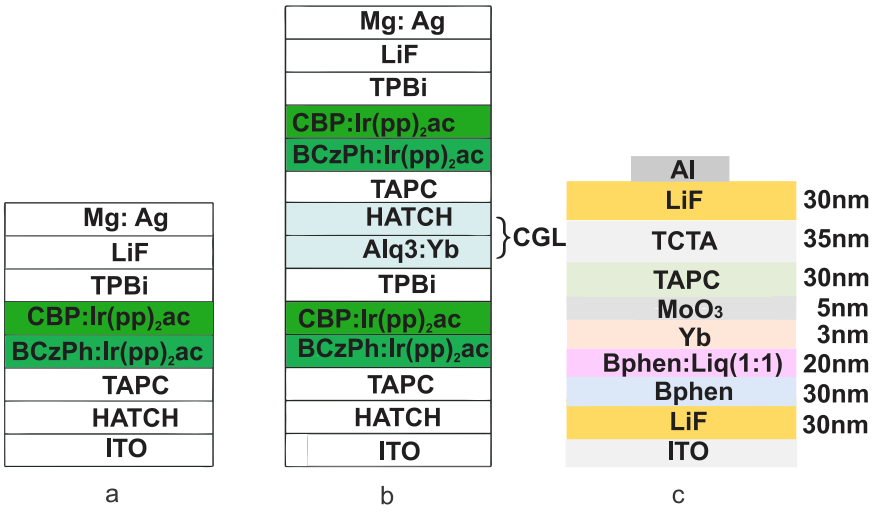

Fig. 21. Structure schematic diagrams of (a) conventional single-unit OLEDs and (b) tandem OLEDs including two EL units and a charge generation layer using Alq3: Yb/HAT-CN.

an initial brightness of 10,000 cd/cm^2, emitting pure green light with high color purity (coordinates (0.27, 0.71)) and the ability to adjust the emission properties by changing the resonator length.

- In Fig. 21, **BCzPh:Ir(pp)$_2$(ac)** is a material used in OLEDs as the emissive layer. BCzPh serves as the host material, being a carbazole derivative structurally modified with phenyl (Ph) groups, which ensures good thermal stability and energy compatibility with dopants like Ir(pp)$_2$(ac). Its primary function is to transfer energy from the host to the dopant.
- **pp** refers to phenylpyridine, which forms strong coordination bonds with iridium. Phenylpyridine is the ligand responsible for light emission in the visible range (green or yellow-green).
- **ac** refers to acetylacetonate, which stabilizes the complex. This material acts as a dopant, meaning it's the active light-emitting component responsible for efficient light emission. This material is popular in OLED research and development, particularly for achieving bright green emission.
- **HAT-CN** stands for 1,4,5,8,9,11-hexaazatriphenylenehexacarbonitrile, an organic material commonly used as a hole injection layer (HIL). It has a high work function and helps effectively inject holes from the anode (such as ITO) into the hole transport layer (HTL). It is used to improve OLED characteristics, such as low operating voltage and high efficiency.
- **TAPC** stands for 1,1-bis[(di-4-tolylamino)phenyl]cyclohexane, a widely used hole-transport material (HTL) in OLEDs. It ensures efficient hole transport from the injection layer (such as HAT-CN) to the emissive layer (EML). TAPC has high thermal stability and is well-suited for use in multilayer OLED structures.
- **TPBi** (1,3,5-tris(N-phenylbenzimidazol-2-yl)benzene) is an organic material used as an electron transport layer (ETL) or blocking layer (EBL) in OLEDs. TPBi has a high vacant orbital energy (LUMO), which makes it effective in transporting electrons to the emissive layer. It is also used to prevent hole leakage from the emissive layer, improving recombination efficiency. These materials play a key role in ensuring high efficiency in OLED devices and optimizing their performance.
- Finally, **LiF** and **Mg:Ag** are critical materials used in OLED structures to enhance charge injection and transport, as well as to form electrodes. As mentioned earlier, LiF is typically applied as a thin layer on the electron transport layer (ETL) before the cathode. It reduces the injection barrier for electrons from the cathode into the transport layer, thereby improving device efficiency. Mg:Ag is an alloy of metals used to form the cathode in OLEDs. It serves as the source of electrons that are injected into the ETL through the LiF layer. Silver (Ag) enhances the stability and conductivity of the cathode, while magnesium (Mg) reduces the work function of the cathode, facilitating easier injection. The alloy typically contains about 10 % silver, which ensures high stability and reduces cathode degradation during OLED operation.

LiF modifies the vacuum energy level of the metal cathode, improving electron injection into the emissive layer. With a high work function (~14 eV), it is effective for electron injection. LiF is used in small concentrations to optimize OLED performance. As a result, LiF enhances electron injection from the metal cathode (e.g., Mg:Ag), reduces the operating voltage of the OLED, and leads to higher overall efficiency. The combination of LiF and Mg:Ag significantly increases the efficiency and stability of OLED devices.

The optimization of LiF use in the charge generation and transport mechanism is a key factor in achieving these results. This represents a significant advancement in the tandem OLED technology utilizing LiF, compared to previous studies.

In the work referenced by [130], a charge generation layer (CGL) with an intermediate layer of ytterbium (Yb) for tandem OLEDs (Fig. 21c) has been developed and studied. Such devices are used to improve the efficiency, stability, and lifespan of OLEDs. Yb outperforms traditional materials, such as aluminum (Al) and silver (Ag), due to its lower optical absorption and better conductivity. The insertion of Yb results in n-type doping, reducing the energy barrier between layers and facilitating electron transport. Since LiF has high dielectric permeability and electrical resistance, double application of LiF on both sides of the CGL prevents charge leakage and reduces the likelihood of electron-hole interactions in adjacent layers (Fig. 21c).

Thus, when comparing different OLED structures (Fig. 21a, b, c), in the first case (Fig. 21a, conventional single-layer OLED), the device has a simpler structure but suffers from high operating voltages and a shorter lifespan. In the second scheme (Fig. 21b, tandem OLED), the LiF layer is used only on one side of the CGL, improving charge transport and reducing operating voltage compared to the first scheme, though the isolation effect of the layers is less pronounced. In the third scheme (Fig. 21c, tandem OLED with double-layer LiF), the double LiF layer combined with the Yb-containing CGL achieves better efficiency and lifespan due to optimized charge distribution, reduced leakage, and improved n-type doping. The advantage of this structure is that, with the double LiF layer and Yb, current efficiency increases as the double LiF layer further stabilizes the charge transport processes due to better electron transport through the CGL and a low injection barrier using Yb. This double-layer LiF scheme demonstrates the highest lifespan (LT50), surpassing the previous schemes.

Thus, the use of a double LiF layer and the introduction of Yb into the CGL structure represents a significant advancement in OLED technology. This solution allows the creation of more stable, durable, and efficient devices that outperform traditional OLEDs in several key parameters, including charge injection efficiency, operating voltages, and emission color characteristics. This design improves the separation of charge carriers and optimizes the device's operation. This technology offers a promising solution for creating highly efficient and long-lasting OLED devices.

Work is also underway on the highly anticipated Micro-LED technology [130], which surpasses OLED devices in terms of color reproduction, contrast, pixel density, energy efficiency, and flexibility due to the individual assembly of tiny LEDs onto a substrate. The Micro-LED technology, a further development of LEDs, is considered the most promising next-generation display technology due to its outstanding brightness, high efficiency, and extremely high performance.

The future of OLED technology in the coming years promises to be exciting thanks to a number of innovations and improvements [125]. One of the key directions will be the enhancement of image quality, including increased brightness, contrast, and expanded color range. Reducing the cost of OLED display production, due to scaling up manufacturing capabilities and improving efficiency, will make the technology more accessible to the mass market. Flexible and foldable OLED displays will become increasingly durable and long-lasting, opening up new opportunities for use in smartphones, tablets, and laptops. Transparent and mirror OLED displays will find applications in the automotive industry, architecture, and retail, providing new solutions for integrating screens into various surfaces. Extending the lifespan of OLED panels and reducing energy consumption will continue to be priorities, allowing for expanded use in desktop monitors and wearable electronics. Advanced technologies such as QD-OLED and Micro-LED will offer improved characteristics, including even greater brightness and longevity, though they remain in the high-price segment for now. Environmental aspects of OLED display production and recycling will also be addressed, reducing their impact on the environment. In the coming years, we can expect new models of OLED displays with enhanced characteristics and new features, making them even more popular and accessible to a wide range of users.

Thus, in OLED structures, LiF is used due to its unique electrical and chemical properties. Its primary application is to improve the efficiency of electron injection into the active layer of the OLED. Lithium fluoride is used as a layer applied to the cathode of the OLED structure. It serves to

enhance the contact between the cathode (usually metals such as aluminum) and the organic layers of the device. LiF has good electron emission properties, which helps reduce the electron injection barrier and improves the device's efficiency. This layer also helps enhance the stability and longevity of OLED elements. Additionally, LiF possesses high chemical stability and can serve as protection against environmental factors, contributing to the durability of OLED devices.

5. Conclusion and future prospective

The review provides a detailed description of a number of unique characteristics of LiF crystals, which are formed due to the physicochemical properties of the crystal, and their influence on technological progress in various fields up to the present day. Fig. 22 illustrates the evolution and expansion of the applications of LiF-based materials from the 1950s to the anticipated future. Fig. 22 shows how the areas of application of LiF have significantly expanded over time, from optical lenses to high-tech fields such as quantum computing and others.

LiF is a unique compound among all known materials due to its largest band gap, which results in high optical transparency and chemical stability. These aspects comprehensively influence the use of this material across a wide range of science and technology Since the 1950s, lithium fluoride has been used in various applications. In Table 10, some of the main areas of application and future prospects for lithium fluoride are collected.

Thus, studying the physical and chemical properties of the subsurface region of LiF is a promising research direction that can lead to the creation of new materials and devices, as well as solving current societal challenges. A sharp increase in the number of publications (threefold by 2025) related to experimental and theoretical studies on the surface of LiF is expected, driven by its growing potential in LIBs, especially as a key component of solid electrolytes. Its high ionic conductivity, chemical stability, and compatibility with other materials make it an ideal candidate for this role. Research in this area is ongoing, and undoubtedly, LiF will be increasingly used in advanced lithium-ion technologies and future generations of batteries.

Based on current trends and conclusions, several promising research directions in the field of LiF can be predicted:

- In-depth studies of the mechanism of ionic conductivity in LiF on solid electrolytes will lead to improved and optimized ionic conductivity and reduced resistance. This will also enhance the stability and compatibility of LiF in contact with other materials, preventing degradation and increasing lifespan. LiF could become a key component in the development of new solid electrolytes for solid-state batteries. Solid electrolytes with LiF additives can provide high ionic conductivity and stability at high temperatures. Lithium fluoride has significant potential for improving lithium-ion battery performance, especially in the context of high-voltage and fast-charging systems. Its use as a coating and electrolyte component can significantly enhance the stability, efficiency, and durability of batteries, making LiF an important material for future energy storage developments.
- Analyzing various types of defects (vacancies, interstitial atoms, dislocations) on the LiF surface will change mechanical and electrochemical properties, which can be manipulated and used in developing new processing methods, nanostructuring, and surface modification of LiF to improve its characteristics, including creating protective layers. In the future, structural defects could become a trigger and key factor in solid-state batteries' failure. Proper management of defects in LiF will lead to the stabilization of high-voltage cathodes, such as LCO, by reducing oxidative reactions at high voltages. This will allow for higher operating voltages and increased energy density of batteries.
- The study of the possibilities of implanting rare earth elements, such as europium or terbium, into the LiF crystal will enable its use in 3D holography of images due to their fluorescent properties.
- Researching the possibilities of using LiF in composite materials, such as polymers, ceramics, and metals, to enhance their strength, stability, and conductivity, will lead to the creation of new materials with unique properties.
- Using advanced molecular dynamics methods and theoretical modeling to predict defect behaviors, such as ion diffusion and interaction with other substances, and their impact on LiF properties.
- Studying LiF's behavior under high temperatures and radiation exposure, its resistance to various types of stresses and deformations, which is important for applications in space technology and nuclear energy.
- Developing methods for recycling and reprocessing LiF after use in devices to minimize environmental impact and reduce production costs, improving LiF's availability for widespread use.

In the future, the results of these studies are mainly important for new types of commercial tomographs using fast electrons [131], for biological, space, and nuclear research. These research directions can lead to significant improvements in lithium-ion battery technology and the creation of new materials with unique properties, which will have a wide range of applications in various industries and technologies. In addition to traditional methods, the use of 3D printers, integration with composite materials, the assistance of artificial intelligence, various simulation programs, and advanced interdisciplinary sciences and technologies will lead to more widespread use of LiF in science and technology.

Ethics approval and consent to participate

Not applicable

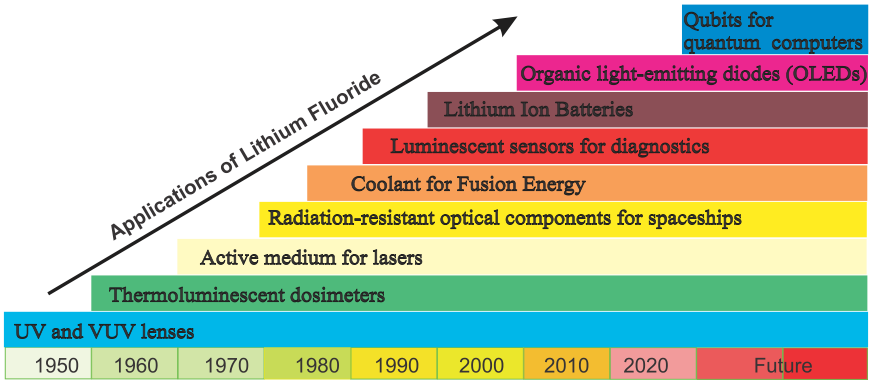

Fig. 22. Evolution and Expansion of the Applications of LiF-Based Materials.

Table 10
Main scientific directions, applications, and prospects for lithium fluoride.

Direction	Application	Future Prospects
Energy	Use of LiF in fluoride melts for cooling in nuclear fusion reactors.	Increase in the efficiency of blanket systems and tritium generation.
	Addition to electrolytes for LIBs.	Improvement in battery stability and longevity.
	Coating of electrodes to reduce side reactions.	Extension of battery life.
Optics and Photonics	Production of lenses, windows, and prisms for UV and vacuum UV spectra.	Application in laser technologies for generating ultrashort pulses.
	Active medium for lasers based on color centers (e.g., F_2, F_3^+).	Use in nonlinear optics and development of compact optical devices.
Radiation Physics	Thermoluminescent dosimeters for radiation measurement.	Improvement of radiation dosimetry in medicine and nuclear facilities.
	Study of radiation defects in LiF.	Development of radiation-resistant materials for extreme conditions.
Materials Science	Study of color centers (F, F_2, F_3^+, F_4) to understand crystal defects.	Creation of new quantum materials for computing and sensors.
	Development of thin-film coatings with high corrosion and radiation resistance.	Application in nanotechnology and microelectronics.
Space Technologies	Production of radiation-resistant optical components for satellites and telescopes.	Use in deep space missions.
	Materials for protective coatings resistant to extreme conditions.	Development of innovative materials for spacecraft.
Quantum Technologies	Color centers (e.g., F_2, F_3^+) as potential qubits for quantum computers.	Advancement of quantum computing and sensors.
Medicine	Luminescent sensors for diagnostics and monitoring.	Enhancement of diagnostic technologies.
	Radiation dose control in radiotherapy due to thermoluminescent properties.	Creation of precise dosimetric devices for medical applications.
Fusion Energy	Use of LiF in blankets for fusion reactors and tritium generation.	Development of safe and efficient systems for fusion energy.
OLED Displays	Use of LiF as a buffer layer in OLED.	Increase in the efficiency and stability of OLEDs for smartphones, TVs, and flexible displays.
	Use in high-quality energy-efficient displays.	Development of bright, durable OLED panels with reduced energy consumption.

Consent for publication

Not applicable

Research involving Human Participants and/or Animals

Not applicable

Informed consent

Not applicable

Funding

This work was supported by ongoing funding from the Academy of Sciences of the Republic of Uzbekistan. No additional grants to carry out or direct this particular research were obtained.

Declaration of Competing Interest

The authors declare that they have no known competing financial interests or personal relationships that could have appeared to influence the work reported in this paper

Appendix A. Supporting information

Supplementary data associated with this article can be found in the online version at doi:10.1016/j.nxmate.2025.100548.

Data availability

The data that support the findings of this study are available from the corresponding author upon reasonable request.

References

[1] H. Zhu, S. Dong, Y. Zhao, P.K. Lee, D.Y.W. Yu, High-performance graphite|| Li4Ti5O12 dual-ion full batteries enabled by in-situ formation of LiF-rich solid electrolyte interphase on Li4Ti5O12 anode, J. Power Sources 592 (2024) 233953, https://doi.org/10.1016/J.JPOWSOUR.2023.233953.

[2] J. Li, Y. Cai, F. Zhang, Y. Cui, W. Fang, H. Da, H. Zhang, S. Zhang, Exceptional interfacial conduction and LiF interphase for ultralong life PEO-based all-solid-state batteries, Nano Energy 118 (2023) 108985, https://doi.org/10.1016/J.NANOEN.2023.108985.

[3] X. Jin, G. Huang, X. Zhao, G. Chen, M. Guan, Y. Li, An in situ LiF-enriched solid electrolyte interphase from CoF2-decorated N-doped carbon for dendrite-free Li metal anodes, Energy Adv. 2 (2023) 725–732, https://doi.org/10.1039/D3YA00035D.

[4] R.C. Palmer, A prototype LiF radiation dosimeter for personnel monitoring, Int. J. Appl. Radiat. Isot. 17 (1966) 413–416, https://doi.org/10.1016/0020-708X(66)90067-6.

[5] C.A.M. Silva, I.R. Magalhães, M. Lorduy-Alós, S. Gallardo, C. Pereira, A.L. Costa, G. Verdú, A neutronic evaluation of a thorium-based molten salt breeder reactor, Nucl. Eng. Des. 421 (2024) 113049, https://doi.org/10.1016/j.nucengdes.2024.113049.

[6] J. Xiao, Z. Deng, A novel white organic electroluminescent device based on a thin LiF interlayer, Synth. Met. 162 (2012) 2016–2019, https://doi.org/10.1016/j.synthmet.2012.09.015.

[7] M. Li, J. Lu, Z. Chen, K. Amine, 30 Years of Lithium-Ion Batteries, Adv. Mater. 30 (2018), https://doi.org/10.1002/adma.201800561.

[8] M.A. Mussaeva, E.M. Ibragimova, S.N. Buzrikov, Optical Spectra of Gamma-Irradiated LiF Crystals with Anisotropic Lithium Nanoparticles, Opt. Spectrosc. (Engl. Transl. Opt. i Spektrosk. 124 (2018) 644–648, https://doi.org/10.1134/S0030400X18050144.

[9] P. Seth, S. Aggarwal, S. Bahl, P. kumar, Optically stimulated luminescence dosimetry on tissue equivalent LiF: Mg, Cu, Na, Si phosphor, Opt. (Stuttg.) 260 (2022) 169060, https://doi.org/10.1016/j.ijleo.2022.169060.

[10] E.M. Ibragimova, M.A. Mussaeva, S.N. Buzrikov, Recombination gamma-luminescence at the nanometal Li - dielectric LiF interfaces, Radiat. Phys. Chem. 111 (2015) 40–45, https://doi.org/10.1016/j.radphyschem.2015.02.009.

[11] R.M. Montereali, Point defects in thin insulating films of lithium fluoride for optical microsystems, in: Handb. Thin Film., Elsevier, 2002, pp. 399–431, https://doi.org/10.1016/B978-012512908-4/50043-6.

[12] M. Puchalska, P. Bilski, P. Olko, Thermoluminescence glow peak parameters for LiF:Mg,Ti with modified activator concentration, Radiat. Meas. 42 (2007) 601–604, https://doi.org/10.1016/j.radmeas.2007.01.081.

[13] C.J. Salas-Juárez, M.A. Ugalde-Valdés, J. Guzmán-Mendoza, D. Nolasco-Altamirano, M. Martínez-Gil, C.E. Gómez-Dominguez, C.A. Guarin, R. Melendrez, T. Rivera-Montalvo, Persistent luminescence of commercial TLD-100 dosimeter: Using shallow traps for radiation dosimetry, Radiat. Meas. 167 (2023) 106997, https://doi.org/10.1016/j.radmeas.2023.106997.

[14] S.W.S. McKeever, Mechanisms of Thermoluminescence Production in Materials for Radiation Dosimetry (INVITED), Radiat. Prot. Dosim. 17 (1986) 431–435, https://doi.org/10.1093/rpd/17.1-4.431.

[15] A. Mitchell, I.G. Hill, A. Syme, Preliminary comparison of organic electret-style devices on silicon and flexible plastic substrates as real-time ionizing radiation dosimeters, Org. Electron. 122 (2023) 106910, https://doi.org/10.1016/j.orgel.2023.106910.

[16] E.M. Abou Hussein, A. Sobhy, Experimental investigation of new rare earth borosilicate glasses from municipal waste ash as high-dose radiation dosimeters, Ceram. Int. 50 (2024) 23012–23024, https://doi.org/10.1016/j.ceramint.2024.04.023.

[17] L. Stolarczyk, Ž. Knežević, N. Adamek, C. Algranati, I. Ambrozova, C. Domingo, V. Dufek, J. Farah, F. Fellin, M. Klodowska, J. Kubancak, M. Liszka, M. Majer, V. Mares, S. Miljanić, O. Ploc, M. Romero-Expósito, K. Schinner, M. Schwarz, S. Trinkl, F. Trompier, M. Wielunski, R. Harrison, P. Olko, Comparison of passive

dosimeters for secondary radiation measurements in scanning proton radiotherapy, Phys. Med. 30 (2014) e65, https://doi.org/10.1016/j.ejmp.2014.07.197.
[18] C. Boronat, V. Correcher, J.C. Bravo-Yagüe, I. Sarasola-Martin, J. Garcia-Guinea, J.F. Benavente, Comparing the effect of electron beam, beta and ultraviolet C exposure on the luminescence emission of commercial dosimeters, Spectrochim. Acta - Part A Mol. Biomol. Spectrosc. 295 (2023) 122571, https://doi.org/10.1016/j.saa.2023.122571.
[19] M. Piccinini, E. Nichelatti, C. Ronsivalle, A. Ampollini, G. Bazzano, F. Bonfigli, P. Nenzi, V. Surrenti, E. Trinca, M. Vadrucci, M.A. Vincenti, L. Picardi, R. M. Montereali, Visible photoluminescence of color centers in LiF crystals for advanced diagnostics of 18 and 27 MeV proton beams, Radiat. Meas. 124 (2019) 59–62, https://doi.org/10.1016/j.radmeas.2019.03.010.
[20] O. Van Hoey, M. De Saint-Hubert, A. Parisi, M.Á. Caballero-Pacheco, C. Domingo, F. Pozzi, R. Froeschl, L. Stolarczyk, P. Olko, Evaluation and modelling of the lithium fluoride based thermoluminescent detector response at the CERN-EU high-energy reference field (CERF), Radiat. Meas. 162 (2023) 106923, https://doi.org/10.1016/j.radmeas.2023.106923.
[21] E. Nichelatti, M. Piccinini, A. Ampollini, L. Picardi, C. Ronsivalle, F. Bonfigli, M. A. Vincenti, R.M. Montereali, Modelling of photoluminescence from F2 and F3+ colour centres in lithium fluoride irradiated at high doses by low-energy proton beams, Opt. Mater. (Amst.). 89 (2019) 414–418, https://doi.org/10.1016/j.optmat.2019.01.052.
[22] R.M. Montereali, A. Ampollini, L. Picardi, C. Ronsivalle, F. Bonfigli, S. Libera, E. Nichelatti, M. Piccinini, M.A. Vincenti, Visible photoluminescence of aggregate colour centres in lithium fluoride thin films for low-energy proton beam radiation detectors at high doses, J. Lumin. 200 (2018) 30–34, https://doi.org/10.1016/j.jlumin.2018.04.005.
[23] M. Leoncini, M.A. Vincenti, F. Bonfigli, S. Libera, E. Nichelatti, M. Piccinini, A. Ampollini, L. Picardi, C. Ronsivalle, A. Mancini, A. Rufoloni, R.M. Montereali, Optical investigation of radiation-induced color centers in lithium fluoride thin films for low-energy proton-beam detectors, Opt. Mater. (Amst.). 88 (2019) 580–585, https://doi.org/10.1016/J.OPTMAT.2018.12.031.
[24] M. Piccinini, C. Ronsivalle, A. Ampollini, G. Bazzano, L. Picardi, P. Nenzi, E. Trinca, M. Vadrucci, F. Bonfigli, E. Nichelatti, M.A. Vincenti, R.M. Montereali, Proton beam spatial distribution and Bragg peak imaging by photoluminescence of color centers in lithium fluoride crystals at the TOP-IMPLART linear accelerator, Nucl. Instrum. Methods Phys. Res. Sect. A Accel. Spectrometers, Detect. Assoc. Equip. 872 (2017) 41–51, https://doi.org/10.1016/j.nima.2017.07.065.
[25] R.M. Montereali, M. Piccinini, A. Ampollini, L. Picardi, C. Ronsivalle, F. Bonfigli, E. Nichelatti, M.A. Vincenti, Visible photoluminescence of color centers in lithium fluoride detectors for low-energy proton beam Bragg curve imaging and dose mapping, Opt. Mater. (Amst.). 95 (2019) 109242, https://doi.org/10.1016/j.optmat.2019.109242.
[26] I. Eliyahu, L. Oster, A. Shapiro, M. Tessler, Y.S. Horowitz, Measurements of the neutron and gamma dose via TL/OSL in LiF:Mg,Ti and activation methods analysis of aluminum foils, Nucl. Instrum. Methods Phys. Res. Sect. B Beam Interact. Mater. At. 552 (2024) 165375, https://doi.org/10.1016/j.nimb.2024.165375.
[27] I. Eliyahu, Y.S. Horowitz, G. Reshes, A. Shapiro, S. Biderman, Y. Assor, D. Ginsburg, B. Herman, L. Oster, Study of thermally and optically stimulated luminescence in LiF:Mg,Ti following neutron and beta irradiation, J. Phys. Conf. Ser. 2298 (2022) 012007, https://doi.org/10.1088/1742-6596/2298/1/012007.
[28] Y.S. Horowitz, L. Oster, I. Eliyahu, The saga of the thermoluminescence (TL) mechanisms and dosimetric characteristics of LiF:Mg,Ti (TLD-100), J. Lumin. 214 (2019) 116527, https://doi.org/10.1016/j.jlumin.2019.116527.
[29] M. Sterenberg, Y.S. Horowitz, L. Oster, I. Eliyahu, G. Reshes, D. Nemirovky, B. Herman, A. Shapiro, S. Biderman, H. Einav, Kinetic modeling of charge transfer following photon bleaching post-irradiation of spatially correlated trapping and luminescent centers in LiF:Mg,Ti, Nucl. Instrum. Methods Phys. Res. Sect. B Beam Interact. Mater. At. 540 (2023) 94–101, https://doi.org/10.1016/j.nimb.2023.04.013.
[30] Y.S. Horowitz, L. Oster, G. Reshes, D. Nemirovsky, D. Ginzburg, S. Biderman, Y. Bokobza, M. Sterenberg, I. Eliyahu, Recent Developments in Computerised Analysis of Thermoluminescence Glow Curves: Software Codes, Mechanisms and Dosimetric Applications, Radiat. Prot. Dosim. 198 (2022) 821–842, https://doi.org/10.1093/rpd/ncac147.
[31] M. Piccinini, E. Nichelatti, G. Esposito, E. Cisbani, F. Santavenere, P. Anello, V. Nigro, M.A. Vincenti, F. Limosani, C. Ronsivalle, A. Ampollini, C. De Angelis, R.M. Montereali, Detection of fluorescent low-energy proton tracks in lithium fluoride crystals, Radiat. Meas. 174 (2024), https://doi.org/10.1016/j.radmeas.2024.107140.
[32] M.A. Vincenti, R.M. Montereali, F. Bonfigli, E. Nichelatti, V. Nigro, M. Piccinini, M. Koenig, P. Mabey, G. Rigon, H.J. Dabrowski, Y. Benkadoum, P. Mercere, P. Da Silva, T. Pikuz, N. Ozaki, S. Makarov, S. Pikuz, B. Albertazzi, Advanced spectroscopic investigation of colour centres in LiF crystals irradiated with monochromatic hard x-rays, J. Phys. Condens. Matter 36 (2024) 205701, https://doi.org/10.1088/1361-648X/ad2796.
[33] R.M. Montereali, V. Nigro, M. Piccinini, M.A. Vincenti, P. Nenzi, C. Ronsivalle, E. Nichelatti, Visible proton Bragg curve imaging by colour centre photoluminescence in radiation detectors based on lithium fluoride films on silica, J. Phys. Condens. Matter 36 (2024) 215703, https://doi.org/10.1088/1361-648X/ad2a08.
[34] M. Sorokin, Z.Z. Malikova, A. Dauletbekova, G. Baubekova, G. Aralbayeva, A. Akilbekov, Thermal annealing of radiation damages produced by swift 14N and 16O ions in LiF crystals, Mater. Res. Express (2024), https://doi.org/10.1088/2053-1591/ad5a68.
[35] M.V. Sorokin, K. Schwartz, V.I. Dubinko, A.N. Khodan, A.K. Dauletbekova, M. V. Zdorovets, Kinetics of lattice defects induced in lithium fluoride crystals during irradiation with swift ions at room temperature, Nucl. Instrum. Methods Phys. Res. Sect. B Beam Interact. Mater. At. 466 (2020) 17–19, https://doi.org/10.1016/j.nimb.2020.01.007.
[36] U.B. Sharopov, B.G. Atabaev, R. Djabberganov, M.K. Kurbanov, Kinetics of aggregations of F 2, F 3, X, and colloid centers in LiF/Si(111) films upon low-temperature annealing, J. Surf. Investig. X-Ray, Synchrotron Neutron Tech. 7 (2013) 195–199, https://doi.org/10.1134/S1027451012120117.
[37] T. Krasta, I. Manika, A. Kuzmin, J. Maniks, R. Grants, A.I. Popov, Effect of ion-induced secondary radiations on the formation of extended defects and radiolysis beyond the range of swift 12C, 50Ti, and 52Cr ions in LiF, Nucl. Instrum. Methods Phys. Res. Sect. B Beam Interact. Mater. At. 545 (2023) 165142, https://doi.org/10.1016/j.nimb.2023.165142.
[38] G. Massillon-Jl, C.S.N. Johnston, L. Stella, J. Kohanoff, Electronic structure calculations of defect states in Ti-doped LiF, Radiat. Meas. 174 (2024) 107114, https://doi.org/10.1016/j.radmeas.2024.107114.
[39] A. Dauletbekova, K. Schwartz, M.V. Sorokin, A. Russakova, M. Baizhumanov, A. Akilbekov, M. Zdorovets, M. Koloberdin, F center creation and aggregation in LiF crystals irradiated with 14N, 40Ar, and 84Kr ions, Nucl. Instrum. Methods Phys. Res. Sect. B Beam Interact. Mater. At. 326 (2014) 311–313, https://doi.org/10.1016/j.nimb.2013.09.026.
[40] A.V. Sorokin, S. Piskunov, I. Isakoviča, I. Makarenko, I. Karbovnyk, A.I. Popov, Raman spectra of vacancy-containing LiF: Predictions from first principles, Nucl. Instrum. Methods Phys. Res. Sect. B Beam Interact. Mater. At. 480 (2020) 33–37, https://doi.org/10.1016/j.nimb.2020.07.025.
[41] A.M. Sadek, N.Y. Abdou, H.A. Alazab, Uncertainty of LiF thermoluminescence at low dose levels: Experimental results, Appl. Radiat. Isot. 185 (2022) 110245, https://doi.org/10.1016/j.apradiso.2022.110245.
[42] U.B. Sharopov, B.G. Atabaev, R. Djabbarganov, M.K. Kurbanov, M.M. Sharipov, Procedure for determining defects in sputtered clusters of ionic crystals, J. Surf. Investig. X-Ray, Synchrotron Neutron Tech. 10 (2016) 245–249, https://doi.org/10.1134/S1027451016010328.
[43] S.G. Gorbics, F.H. Attix, LiF and CaF2:Mn thermoluminescent dosimeters in tandem, Int. J. Appl. Radiat. Isot. 19 (1968) 81–84, https://doi.org/10.1016/0020-708X(68)90074-4.
[44] S.B. Almeida, D. Villani, R.K. Sakuraba, A.C.P. Rezende, L.L. Campos, Dosimetric evaluation and comparation of TL responses of LiF:Mg,Ti and μLiF:Mg,Ti in the clinical electron beams dosimetry applied to total skin irradiation (TSEB) treatments, Radiat. Meas. 125 (2019) 15–18, https://doi.org/10.1016/j.radmeas.2019.03.007.
[45] S. Zhang, K. Tang, H. Fan, L. Fu, A competitive radioluminescence material - LiF: Mg,Cu,P for real-time dosimetry, Radiat. Meas. 151 (2022) 106719, https://doi.org/10.1016/j.radmeas.2022.106719.
[46] I. Karachalios, D. Mathes, I. Valais, I. Vamvakas, I. Sianoudis, Development of a timing control system for laser induced fluorescence (LIF) in medical applications, Phys. Med. 30 (2014) e97, https://doi.org/10.1016/j.ejmp.2014.07.277.
[47] A.S. Pradhan, Fast-neutron response of sensitized LiF TLD-700, Int. J. Radiat. Appl. Instrum. Part. 13 (1987) 111–113, https://doi.org/10.1016/1359-0189(87)90020-3.
[48] S. Lee, J. Lee, G. Kim, S.J. Ye, Estimating 10B and 14N doses using a pair of LiF-based TLD-600 and TLD-700 as an alternative to gold activation method, Nucl. Instrum. Methods Phys. Res. Sect. A Accel. Spectrometers, Detect. Assoc. Equip. 1050 (2023) 168141, https://doi.org/10.1016/j.nima.2023.168141.
[49] A.I. Castro-Campoy, C. Cruz-Vázquez, R. Pérez-Salas, V.M. Castaño, R. Bernal, Novel non-thermoluminescent CaSO4:Dy dosimeters, Appl. Radiat. Isot. 217 (2025) 111606, https://doi.org/10.1016/j.apradiso.2024.111606.
[50] U.B. Sharopov, K. Kaur, M.K. Kurbanov, D.S. Saidov, S.R. Nurmatov, M. M. Sharipov, B.E. Egamberdiev, Comparison of electron irradiation on the formation of surface defects in situ and post thin-film LiF/Si(111) deposition, Thin Solid Films 735 (2021) 138902, https://doi.org/10.1016/j.tsf.2021.138902.
[51] U. Sharopov, Surface Defects in Wide-Bandgap LiF, SiO2, and ZnO Crystals, Springer Nature Switzerland, Cham, 2024, https://doi.org/10.1007/978-3-031-58850-1.
[52] U. Sharopov, U. Gopparov, K. Rashidov, K. Kaur, M. Kurbanov, T. Juraev, B. Egamberdiev, A. Kakhramonov, S. Turopova, D. Saidov, B. Sanat, Formation of defects on the surface of LiF crystals under irradiation with different ions mass, Radiat. Eff. Defects Solids 178 (2023) 539–552, https://doi.org/10.1080/10420150.2022.2133716.
[53] U. Sharopov, K. Kaur, M. Kurbanov, N. Avezov, T. Juraev, B. Egamberdiev, K. Rashidov, D. Turapova, Influence of the irradiation of ions of different mass on the formation of surface defects of lithium fluoride thin films, Surf. Interface Anal. 54 (2022) 1052–1059, https://doi.org/10.1002/sia.7130.
[54] G.D. Rosales, A.C. Resentera, G.J. Fino, E.G. Pinna, M.H. Rodriguez, Optimization of LiF dissolution with Al2(SO4)3 and its application to lithium extraction by fluorination of α-spodumene, Hydrometallurgy 227 (2024) 106336, https://doi.org/10.1016/j.hydromet.2024.106336.
[55] J. Farahbakhsh, F. Arshadi, Z. Mofidi, M. Mohseni-Dargah, C. Kök, M. Assefi, A. Soozanipour, M. Zargar, M. Asadnia, Y. Boroumand, V. Presser, A. Razmjou, Direct lithium extraction: A new paradigm for lithium production and resource utilization, Desalination 575 (2024) 117249, https://doi.org/10.1016/j.desal.2023.117249.

[56] R. Dong, J. Shi, Y. Li, W. Tian, X. Liu, Dielectric energy storage properties of low-temperature sintered BNT-based ceramics with LiF and B2O3–Bi2O3 as sintering aids, Ceram. Int. (2024), https://doi.org/10.1016/j.ceramint.2024.01.187.
[57] Z. Xiao, L. Jiang, L. Song, T. Zhao, M. Xiao, Q. Yan, L. Li, Research progress on interfacial problems and solid-state electrolytes in lithium batteries, J. Energy Storage 96 (2024) 112696, https://doi.org/10.1016/j.est.2024.112696.
[58] C. Griffard, S.G. Penoncello, J.C. Crepeau, Use of the Soft-Sphere Equation of State to predict the thermodynamic properties of the molten salt mixtures LiF-BeF2, NaF-BeF2, and KF-BeF2, Prog. Nucl. Energy 68 (2013) 188–199, https://doi.org/10.1016/j.pnucene.2013.06.008.
[59] K. Lipkina, K. Palinka, E. Geiger, B.W.N. Fitzpatrick, O.S. Vălu, O. Beneš, M.H. A. Piro, Thermodynamic investigations of the LiF-CsF and NaF-CsF pseudo-binary systems, J. Nucl. Mater. 568 (2022) 153901, https://doi.org/10.1016/j.jnucmat.2022.153901.
[60] K. Zeng, Q. Liu, H. Ma, G. Zhao, Q. An, C. Zhang, Y. Yang, M. Sun, Q. Xu, L. Duan, H. Guo, In situ co-growth LiF-Li3N rich dual-protective layers enable high interface stability for solid-state lithium-metal batteries, Energy Storage Mater. 70 (2024) 103564, https://doi.org/10.1016/j.ensm.2024.103564.
[61] U. Sharopov, A. Abdusalomov, A. Kakhramonov, K. Rashidov, F. Akbarova, S. Turapova, M. Kurbanov, D. Saidov, B. Egamberdiev, A. Komolov, S. Pshenichnyuk, K. Kaur, H. Bandarenka, Comparative research fluorine and colloidal aggregate formation on the surface lithium fluoride thin films during electronic, ionic and thermal treatments, Vacuum 213 (2023) 112133, https://doi.org/10.1016/j.vacuum.2023.112133.
[62] Y. Xia, X. Han, Y. Ji, S. Zhang, S. Wei, Y. Gong, J. Yue, Y. Wang, X. Li, Z. Fang, C. Zhao, J. Liang, Solid-electrolyte interphases for all-solid-state batteries, ChemPhysMater (2024), https://doi.org/10.1016/j.chphma.2024.09.006.
[63] M. Nie, D. Chalasani, D.P. Abraham, Y. Chen, A. Bose, B.L. Lucht, Lithium ion battery graphite solid electrolyte interphase revealed by microscopy and spectroscopy, J. Phys. Chem. C. 117 (2013) 1257–1267, https://doi.org/10.1021/jp3118055.
[64] S.K. Heiskanen, J. Kim, B.L. Lucht, Generation and Evolution of the Solid Electrolyte Interphase of Lithium-Ion Batteries, Joule 3 (2019) 2322–2333, https://doi.org/10.1016/j.joule.2019.08.018.
[65] J. Mu, S. Liao, L. Shi, B. Su, F. Xu, Z. Guo, H. Li, F. Wei, Solid-state polymer electrolytes in lithium batteries: latest progress and perspective, Polym. Chem. 22 (2024) 473–499, https://doi.org/10.1039/d3py01311a.
[66] D. Zhang, P. Lv, W. Qin, Y. He, Ultrathin LiF-rich solid electrolyte interphase for stable long-life cycling stabilization of lithium metal anodes, Electrochim. Acta 490 (2024) 144224, https://doi.org/10.1016/j.electacta.2024.144224.
[67] G. Qin, J. Zhang, H. Chen, H. Li, J. Hu, Q. Chen, G. Hou, Y. Tang, Lithium difluoro (oxalate)borate as electrolyte additive to form uniform, stable and LiF-rich solid electrolyte interphase for high performance lithium ion batteries, Surf. Interfaces 48 (2024) 104297, https://doi.org/10.1016/j.surfin.2024.104297.
[68] Y. Huang, Z. Qin, Y. Xie, X. Ma, N. Wang, D. Qian, G. He, L. Wan, X. Meng, In-situ constructed a cross-linking Li3N-LiF network inducing stable cathode/electrolyte interphase for hybrid solid-state lithium batteries, Scr. Mater. 251 (2024) 116191, https://doi.org/10.1016/j.scriptamat.2024.116191.
[69] L. Zhang, M. Bai, Z. Huang, B. Hong, Y. Lai, The critical role of in-situ lithium fluoride in gel polymer electrolyte for high-performance rechargeable batteries, Solid State Ion. 406 (2024) 116461, https://doi.org/10.1016/j.ssi.2024.116461.
[70] Q. Wang, X. He, X. Fan, Y. Ma, Y. Su, D. Zhang, Z. Li, H. Sun, Q. Sun, B. Wang, L. Z. Fan, Enhancing stable LiF-rich interface formation of polyester based electrolyte using fluoroethylene carbonate for quasi-solid state lithium metal batteries, Int. J. Hydrog. Energy 67 (2024) 608–617, https://doi.org/10.1016/j.ijhydene.2024.04.154.
[71] J. Lu, B. Sheng, M. Chen, M. Xu, Y. Zhang, S. Zhao, Q. Zhou, C. Li, B. Wang, J. Liu, J. Chen, Z. Lou, X. Han, Localized high concentration polymer electrolyte enabling room temperature solid-state lithium metal batteries with stable LiF-rich interphases, Energy Storage Mater. 71 (2024) 103570, https://doi.org/10.1016/j.ensm.2024.103570.
[72] Z.Z. Khoo, N.M. Huang, B. Chen, W.G. Chong, High ionic conducting lithium fluoride rich solid electrolyte interphase induced by polysulfide for carbon-based dual ion batteries, Mater. Today Commun. 38 (2024) 108502, https://doi.org/10.1016/j.mtcomm.2024.108502.
[73] J. Sun, H. Yuan, J. Yang, Y.-W. Zhang, J. Wang, Electrolytes for better and safer batteries: Liquid, solid or frameworked, what's next? Mater 1 (2023) 100024 https://doi.org/10.1016/j.nxmate.2023.100024.
[74] H. Al-Salih, E. Baranova, Y. Abu-Lebdeh, Solid-state batteries: The interfacial challenge to replace liquid electrolytes, in: Encycl. Solid-Liquid Interfaces, Elsevier, 2023, pp. V3-444–V3-453, https://doi.org/10.1016/B978-0-323-85669-0.00146-X.
[75] C. Zhang, Y. Zheng, J. Jing, Y. Liu, H. Huang, A comparative LCA study on aluminum electrolytic capacitors: From liquid-state electrolyte, solid-state polymer to their hybrid, J. Clean. Prod. 375 (2022) 134044, https://doi.org/10.1016/j.jclepro.2022.134044.
[76] A. Saleem, L.L. Shaw, R. Iqbal, A. Hussain, A.R. Akbar, B. Jabar, S. Rauf, M. K. Majeed, Ni-rich cathode evolution: exploring electrochemical dynamics and strategic modifications to combat degradation, Energy Storage Mater. 69 (2024) 103440, https://doi.org/10.1016/j.ensm.2024.103440.
[77] G. Wang, Z. Bi, A. Zhang, P. Das, H. Lin, Z.S. Wu, High-Voltage and Fast-Charging Lithium Cobalt Oxide Cathodes: From Key Challenges and Strategies to Future Perspectives, Engineering (2024), https://doi.org/10.1016/j.eng.2023.08.021.
[78] M. Wu, M. Li, Y. Jin, X. Chang, X. Zhao, Z. Gu, G. Liu, X. Yao, In situ formed LiF-Li3N interface layer enables ultra-stable sulfide electrolyte-based all-solid-state lithium batteries, J. Energy Chem. 79 (2023) 272–278, https://doi.org/10.1016/j.jechem.2023.01.007.
[79] S. Liu, X. Shen, L. Wei, R. Wang, B. Ding, J. Yu, J. Yan, Molecular coordination induced high ionic conductivity of composite electrolytes and stable LiF/Li3N interface in long-term cycling all-solid-state lithium metal batteries, Energy Storage Mater. 59 (2023) 102773, https://doi.org/10.1016/j.ensm.2023.102773.
[80] C. Liu, Z. Yang, J. Sun, Synergistic strategy of the phosphorus anode decorated by LiF and combined with KFSI-based electrolyte against shuttle effect of dissoluble polyphosphides for boosting potassium-storage performance, Energy Storage Mater. 53 (2022) 22–31, https://doi.org/10.1016/j.ensm.2022.08.050.
[81] X. Shi, Y. Pang, B. Wang, H. Sun, X. Wang, Y. Li, J. Yang, H.W. Li, S. Zheng, In situ forming LiF nanodecorated electrolyte/electrode interfaces for stable all-solid-state batteries, Mater. Today Nano. 10 (2020) 100079, https://doi.org/10.1016/j.mtnano.2020.100079.
[82] S. Bag, C. Zhou, P.J. Kim, V.G. Pol, V. Thangadurai, LiF modified stable flexible PVDF-garnet hybrid electrolyte for high performance all-solid-state Li–S batteries, Energy Storage Mater. 24 (2020) 198–207, https://doi.org/10.1016/j.ensm.2019.08.019.
[83] J. Tan, J. Matz, P. Dong, J. Shen, M. Ye, A Growing Appreciation for the Role of LiF in the Solid Electrolyte Interphase, Adv. Energy Mater. 11 (2021), https://doi.org/10.1002/aenm.202100046.
[84] Z. Li, L. Wang, X. Huang, X. He, Unveiling the Mystery of LiF within Solid Electrolyte Interphase in Lithium Batteries, Small 20 (2024), https://doi.org/10.1002/smll.202305429.
[85] T. Liu, L. Lin, X. Bi, L. Tian, K. Yang, J. Liu, M. Li, Z. Chen, J. Lu, K. Amine, K. Xu, F. Pan, In situ quantification of interphasial chemistry in Li-ion battery, Nat. Nanotechnol. 14 (2019) 50–56, https://doi.org/10.1038/s41565-018-0284-y.
[86] Y. Zhou, M. Su, X. Yu, Y. Zhang, J.G. Wang, X. Ren, R. Cao, W. Xu, D.R. Baer, Y. Du, O. Borodin, Y. Wang, X.L. Wang, K. Xu, Z. Xu, C. Wang, Z. Zhu, Real-time mass spectrometric characterization of the solid–electrolyte interphase of a lithium-ion battery, Nat. Nanotechnol. 15 (2020) 224–230, https://doi.org/10.1038/s41565-019-0618-4.
[87] H. Yang, B. Zhang, M. Jing, X. Shen, L. Wang, H. Xu, X. Yan, X. He, In Situ Catalytic Polymerization of a Highly Homogeneous PDOL Composite Electrolyte for Long-Cycle High-Voltage Solid-State Lithium Batteries, Adv. Energy Mater. 12 (2022), https://doi.org/10.1002/aenm.202201762.
[88] Q. Ren, Q. Wang, L. Su, G. Liu, Y. Song, X. Shangguan, F. Li, Inorganic/organic composite fluorinated interphase layers for stabilizing ether-based electrolyte in high-voltage lithium metal batteries, J. Mater. Chem. A. 12 (2023) 1072–1080, https://doi.org/10.1039/d3ta05506j.
[89] R. Li, J. Li, L. xin Li, H. Yang, G. Zhang, J. Xiang, X. qian Shen, M. xiang Jing, A bifunctional composite artificial solid electrolyte interphase for high stable solid-state lithium batteries, Colloids Surf. A Physicochem. Eng. Asp. 657 (2023) 130600, https://doi.org/10.1016/j.colsurfa.2022.130600.
[90] H. Yang, M. Jing, L. Wang, H. Xu, X. Yan, X. He, PDOL-Based Solid Electrolyte Toward Practical Application: Opportunities and Challenges, Nano-Micro Lett. 16 (2024) 127, https://doi.org/10.1007/s40820-024-01354-z.
[91] Z. hao Huang, M. xiang Jing, P. qin Wang, W. wen Shao, Z. peng Zhang, G. Zhang, X. qian Shen, A high ionic conductive PDOL/LAGP composite solid electrolyte film for Interfacial Stable solid-state lithium batteries, Ceram. Int. 49 (2023) 5510–5517, https://doi.org/10.1016/j.ceramint.2022.10.074.
[92] H. fei Wu, R. Li, J. xuan Li, L. ping Zhou, Y. Liu, G. Zhang, M. xiang Jing, An in-situ synergistic enhancement strategy from g-C3N4 and PDOL composite solid electrolyte on the interface stability of solid-state lithium battery, Surf. Interfaces 46 (2024) 104048, https://doi.org/10.1016/j.surfin.2024.104048.
[93] Q. Gao, D. Wu, Z. Wang, P. Lu, X. Zhu, T. Ma, M. Yang, L. Chen, H. Li, F. Wu, Superior lithium-metal all-solid-state batteries with in-situ formed Li3N-LiF-rich interphase, Energy Storage Mater. 63 (2023) 103007, https://doi.org/10.1016/J.ENSM.2023.103007.
[94] X. Zhou, C. Li, B. Zhang, F. Huang, P. Zhou, X. Wang, Z. Ma, Difunctional NH2-modified MOF supporting plentiful ion channels and stable LiF-rich SEI construction via organocatalysis for all-solid-state lithium metal batteries, J. Mater. Sci. Technol. 136 (2023) 140–148, https://doi.org/10.1016/J.JMST.2022.07.017.
[95] X. Hu, Y. Li, J. Liu, Z. Wang, Y. Bai, J. Ma, Constructing LiF/Li2CO3-rich heterostructured electrode electrolyte interphases by electrolyte additive for 4.5 V well-cycled lithium metal batteries, Sci. Bull. 68 (2023) 1295–1305, https://doi.org/10.1016/J.SCIB.2023.05.010.
[96] D. Ding, H. Ma, H. Tao, X. Yang, L.Z. Fan, Stabilizing a Li1.3Al0.3Ti1.7(PO4)3/Li metal anode interface in solid-state batteries with a LiF/Cu-rich multifunctional interlayer, Chem. Sci. 15 (2024) 3730–3740, https://doi.org/10.1039/D3SC06347J.
[97] Q. Fan, W. Zhang, Y. Jin, D. Zhang, X. Meng, W. Peng, J. Wang, J. Mo, K. Liu, L. Liu, M. Li, In-situ construction of Li-Ag/LiF composite layer for long cycled all-solid-state Li metal battery, Chem. Eng. J. 477 (2023) 147179, https://doi.org/10.1016/J.CEJ.2023.147179.
[98] S. Zhou, X. Zhang, Nuclear energy development in China: A study of opportunities and challenges, Energy 35 (2010) 4282–4288, https://doi.org/10.1016/j.energy.2009.04.020.
[99] D. Luan, F. Yang, M. Hafeez, Natural resources and nuclear energy development: Does political stability matter? Nucl. Eng. Technol. (2024) https://doi.org/10.1016/j.net.2024.11.030.
[100] M.M. Rahman, J. Dongxu, N. Jahan, M. Salvatores, J. Zhao, Design concepts of supercritical water-cooled reactor (SCWR) and nuclear marine vessel: A review, Prog. Nucl. Energy 124 (2020) 103320, https://doi.org/10.1016/j.pnucene.2020.103320.

[101] Q. Lu, Y. Liu, J. Deng, X. Luo, Z. Deng, Z. Mi, Review of interdisciplinary heat transfer enhancement technology for nuclear reactor, Ann. Nucl. Energy 159 (2021) 108302, https://doi.org/10.1016/j.anucene.2021.108302.
[102] S. Shi, Y. Liu, I. Yilgor, P. Sabharwall, A two-phase three-field modeling framework for heat pipe application in nuclear reactors, Ann. Nucl. Energy 165 (2022) 108770, https://doi.org/10.1016/j.anucene.2021.108770.
[103] S. Qi, B. Han, X. Zhu, B.W. Yang, T. Xing, A. Liu, S. Liu, Machine learning in critical heat flux studies in nuclear systems: A detailed review, Prog. Nucl. Energy 179 (2025) 105535, https://doi.org/10.1016/j.pnucene.2024.105535.
[104] J.E. Kelly, Generation IV International Forum: A decade of progress through international cooperation, Prog. Nucl. Energy 77 (2014) 240–246, https://doi.org/10.1016/j.pnucene.2014.02.010.
[105] Y. Zhang, W. Li, Q. Yu, Development Prospect and Application of Nuclear District Heating in China, : Springe Proc. Phys. (2023) 8–17, https://doi.org/10.1007/978-981-99-1023-6_2.
[106] G. Li, X. Wang, B. Liang, X. Li, B. Zhang, Y. Zou, Modeling and control of nuclear reactor cores for electricity generation: A review of advanced technologies, Renew. Sustain. Energy Rev. 60 (2016) 116–128, https://doi.org/10.1016/j.rser.2016.01.116.
[107] S.P. Tuler, T. Webler, The challenge of community acceptance of small nuclear reactors, Energy Res. Soc. Sci. 118 (2024) 103831, https://doi.org/10.1016/j.erss.2024.103831.
[108] R.O. Scarlat, M.R. Laufer, E.D. Blandford, N. Zweibaum, D.L. Krumwiede, A. T. Cisneros, C. Andreades, C.W. Forsberg, E. Greenspan, L.W. Hu, P.F. Peterson, Design and licensing strategies for the fluoride-salt-cooled, high-temperature reactor (FHR) technology, Prog. Nucl. Energy 77 (2014) 406–420, https://doi.org/10.1016/j.pnucene.2014.07.002.
[109] Y. Zhang, Advanced nuclear power engine: A brief overview of gas core reactor for space exploration, Int. J. Adv. Nucl. React. Des. Technol. 5 (2023) 53–71, https://doi.org/10.1016/j.jandt.2023.05.001.
[110] E.J.T. Berg, A. Buijs, Evaluation framework for molten salt reactors and other new nuclear power reactor systems, Nucl. Eng. Des. 429 (2024) 113588, https://doi.org/10.1016/j.nucengdes.2024.113588.
[111] R.C. Briant, A.M. Weinberg, Molten Fluorides as Power Reactor Fuels, Nucl. Sci. Eng. 2 (1957) 797–803, https://doi.org/10.13182/nse57-a35494.
[112] H.G. MacPherson, Molten Salt Reactor Adventure, Nucl. Sci. Eng. 90 (1985) 374–380, https://doi.org/10.13182/NSE90-374.
[113] A.L. Smith, Structure-property relationships in actinide containing molten salts – A review: Understanding and modelling the chemistry of nuclear fuel salts, J. Mol. Liq. 360 (2022) 119426, https://doi.org/10.1016/j.molliq.2022.119426.
[114] D. Zhang, X. Li, D. Jiang, X. Zhou, X. Lv, S. Yun, W. Wu, X. He, H. Li, X. Min, K. Chen, W. Tian, S. Qiu, G.H. Su, Q. Zhao, Y. Fu, C. Tang, W. Zhuo, J. Li, J. Zuo, Fluoride-Salt-cooled high-Temperature Advanced Reactor (FuSTAR): An integrated nuclear-based energy production and conversion system, Energy 290 (2024) 130048, https://doi.org/10.1016/j.energy.2023.130048.
[115] M.H. Subki, Water cooled small modular reactors (Integral PWR and BWR), in: Encycl. Nucl. Energy, Elsevier, 2021, pp. 694–710, https://doi.org/10.1016/b978-0-12-819725-7.00208-7.
[116] M.A. Amidu, S.A. Olatubosun, A. Ayodeji, Y. Addad, Severe accident in high-power light water reactors: Mitigating strategies, assessment methods and research opportunities, Prog. Nucl. Energy 143 (2022) 104062, https://doi.org/10.1016/j.pnucene.2021.104062.
[117] G. Vaidyanathan, Decay heat removal in sodium cooled fast Reactors-An overview, Ann. Nucl. Energy 205 (2024) 110554, https://doi.org/10.1016/j.anucene.2024.110554.
[118] Y. Dai, X. Zheng, P. Ding, Review on sodium corrosion evolution of nuclear-grade 316 stainless steel for sodium-cooled fast reactor applications, Nucl. Eng. Technol. 53 (2021) 3474–3490, https://doi.org/10.1016/j.net.2021.05.021.
[119] Q. Huang, S. Peng, J. Deng, H. Zeng, Z. Zhang, Y. Liu, P. Yuan, A review of the application of artificial intelligence to nuclear reactors: Where we are and what's next, Heliyon 9 (2023) e13883, https://doi.org/10.1016/j.heliyon.2023.e13883.
[120] M. Wang, H. Ju, J. Wu, H. Qiu, K. Liu, W. Tian, G.H. Su, A review of CFD studies on thermal hydraulic analysis of coolant flow through fuel rod bundles in nuclear reactor, Prog. Nucl. Energy 171 (2024) 105175, https://doi.org/10.1016/j.pnucene.2024.105175.
[121] Y. Deng, C. Liu, B. Pang, B. Qiu, Y. Yin, Y. Wu, Grid-to-rod fretting in nuclear power reactors: Driving mechanisms, research methodologies and mitigation measures, J. Nucl. Mater. 587 (2023) 154705, https://doi.org/10.1016/j.jnucmat.2023.154705.
[122] R. Jayabal, Next-generation solutions for water sustainability in nuclear power plants: Innovations and challenges, Nucl. Eng. Des. 432 (2025) 113757, https://doi.org/10.1016/j.nucengdes.2024.113757.
[123] J.N. Emerson, E.H. Marrero-Jackson, G.A. Nemets, M.A. Okuniewski, J.P. Wharry, Nuclear Reactor Pressure Vessel Welds: A Critical and Historical Review of Microstructures, Mechanical Properties, Irradiation Effects, and Future Opportunities, Mater. Des. 244 (2024) 113134, https://doi.org/10.1016/j.matdes.2024.113134.
[124] C.W. Tang, S.A. Vanslyke, Organic electroluminescent diodes, Appl. Phys. Lett. 51 (1987) 913–915, https://doi.org/10.1063/1.98799.
[125] M. Sarma, L.M. Chen, Y.S. Chen, K.T. Wong, Exciplexes in OLEDs: Principles and promises, Mater. Sci. Eng. R. Rep. 150 (2022) 100689, https://doi.org/10.1016/j.mser.2022.100689.
[126] D. Nayak, R.B. Choudhary, A survey of the structure, fabrication, and characterization of advanced organic light emitting diodes, Microelectron. Reliab. 144 (2023) 114959, https://doi.org/10.1016/j.microrel.2023.114959.
[127] Q. Yang, F. Qian, G. Gou, T. Wang, Y. Duan, C. Lu, G. Wang, L. Duan, W. Yang, Y. Zhang, P. Yang, Performance optimization of green tandem OLEDs with double emitting layers, J. Lumin. 275 (2024) 120798, https://doi.org/10.1016/j.jlumin.2024.120798.
[128] H. Sun, Q. Guo, D. Yang, Y. Chen, J. Chen, D. Ma, High efficiency tandem organic light emitting diode using an organic heterojunction as the charge generation layer: An investigation into the charge generation model and device performance, ACS Photonics 2 (2015) 271–279, https://doi.org/10.1021/acsphotonics.5b00010.
[129] Y. Liu, X. Wu, Z. Xiao, J. Gao, J. Zhang, H. Rui, X. Lin, N. Zhang, Y. Hua, S. Yin, Highly efficient tandem OLED based on C 60 /rubrene: MoO 3 as charge generation layer and LiF/Al as electron injection layer, Appl. Surf. Sci. 413 (2017) 302–307, https://doi.org/10.1016/j.apsusc.2017.04.038.
[130] K. Kim, J.I. Yoo, S.C. Kang, H.Bin Kim, E. young Choi, S. Parani, J.K. Song, Charge generation layer with Yb assistant interlayer for tandem organic light-emitting diodes, Displays 82 (2024) 102656, https://doi.org/10.1016/j.displa.2024.102656.
[131] A. Bieberle, D. Windisch, K. Iskander, M. Bieberle, U. Hampel, A smart multi-plane detector design for ultrafast electron beam x-ray computed tomography, Sens. (Switz.) 20 (2020) 1–16, https://doi.org/10.3390/s20185174.